

**University of Kassel**  
**Faculty of Organic Agricultural Sciences**  
**Department of Grassland Science and Renewable Plant Resources**

**Determination of yield and quality parameters of energy crops applying laboratory and field spectroscopy**

**Doctoral thesis**

tendered by

**Daniela Perbandt**

born in Seesen

Witzenhausen, 2009



## **Danksagung**

Die hier vorliegende Arbeit wäre ohne die Hilfe und Unterstützung einer großen Anzahl von Menschen nicht so geworden wie ich sie heute präsentieren kann.

Damit ich auch niemanden vergesse, möchte ich mich in chronologischer Reihenfolge bei allen bedanken, die wesentlichen Anteil an dieser Arbeit hatten:

Zu allererst meinen Eltern, Hannelore und Rolf, die mich ausprobieren ließen.

Dr. Torsten Zeller, der mich lehrte, dass Wissenschaft kein Urlaubserlebnis ist.

Prof. Michael Wachendorf, der mir die Möglichkeit gab, in einem für mich neuen Fachgebiet zu promovieren; der mich jederzeit unterstützte und von dessen Erfahrung und Sachkenntnis ich sehr profitierte.

Dr. Reinhold Stülpnagel und Thomas Fricke, die durch ihre Expertise, ihren Ideenreichtum und ständiges kritisches Hinterfragen mich oft forderten und meine Arbeit dadurch verbesserten.

Meinen Kollegen, Andrea Gerke, Margit Rode, Wolfgang Funke und Manfred Ellrich, für ihre tatkräftige Unterstützung im Labor und auf dem Feld.

Meinen Kolleginnen, Dr. Sonja Biewer und Dr. Maike Himstedt, für die gemeinsame durch gestandene Zeit und dafür, dass ich immer fragen konnte, wenn mir Fachwissen fehlte.

Zu guter Letzt meinem Mann Christian und meinem Sohn Benedikt, die mich in all der Zeit unterstützten, an mich glaubten und meine Arbeit zu einem Teil mit lebten.

This work has been accepted by the Faculty of Organic Agricultural Sciences of the University of Kassel as a thesis for acquiring the academic degree of Doktor der Agrarwissenschaften (Dr. agr.).

1. Supervisor: Prof. Dr. Michael Wachendorf
2. Supervisor: Prof. Dr. Bernard Ludwig

Defence day: 8. January 2010

#### Eidesstattliche Erklärung

Hiermit versichere ich, dass ich die vorliegende Dissertation selbständig und ohne unerlaubte Hilfe angefertigt und andere als die in der Dissertation angegebenen Hilfsmittel nicht benutzt habe. Alle Stellen, die wörtlich oder sinngemäß aus veröffentlichten oder unveröffentlichten Schriften entnommen sind, habe ich als solche kenntlich gemacht. Kein Teil dieser Arbeit ist in einem anderen Promotions- oder Habilitationsverfahren verwendet worden.

## **Preface**

This thesis is submitted to the Faculty of Organic Agricultural Sciences of the University of Kassel to fulfil the requirements for the degree Doktor der Agrarwissenschaften (Dr. agr.).

This dissertation is based on three papers as first author, which are published or submitted to international refereed journals. They are included in chapter 4, 5 and 6.

Chapter 1 gives the introduction to all parts of the thesis. Chapter 2 contains the objectives of the work and chapter 3 gives an overview of the basic principles of spectroscopy.

Chapter 7 considers the results of the chapters 4, 5 and 6 in a general discussion. A general conclusion and the summary is given in chapter 8 and chapter 9.

The following papers contribute to this thesis:

Chapter 4:

Perbandt, D., Reulein, J., Richter, F., Stülpnagel, R., Wachendorf, M. 2009. Assessment of mass flows and fuel quality during mechanical dehydration of silages using near infrared reflectance spectroscopy. *Bioenergy Research*, Online first. DOI 10.1007/s12155-009-9062-x

Chapter 5:

Perbandt, D., Fricke, T., Wachendorf, M. 2009. Effects of changing sky cover on hyperspectral reflectance measurements for dry matter yield and forage quality prediction. *Computers and Electronics in Agriculture*, submitted.

Chapter 6:

Perbandt, D., Fricke, T., Wachendorf, M. 2009. Off-nadir hyperspectral measurements in maize. Comparison of angle-height combinations for on-the-go-solutions to predict DM yield, protein and ME contents. *Precision Agriculture*, submitted.

**Table of contents**

1	General introduction .....	1
2	Research objectives.....	3
3	Basic principles of spectroscopy.....	4
3.1	<i>The Beer-Lambert Law</i> .....	4
3.2	<i>Specific spectral characteristics of green vegetation</i> .....	5
4	Assessment of mass flows and fuel quality during mechanical dehydration of silages using near infrared reflectance spectroscopy .....	8
4.1	<i>Introduction</i> .....	9
4.2	<i>Material and Methods</i> .....	12
4.2.1	Samples .....	12
4.2.2	Reference analysis .....	13
4.2.3	Mass flow calculations.....	13
4.2.4	NIRS measurement .....	14
4.2.5	Spectra pre-processing .....	14
4.2.6	Calibration .....	15
4.2.7	Validation.....	16
4.3	<i>Results</i> .....	16
4.4	<i>Discussion</i> .....	19
4.4.1	Prediction accuracy for solid fuel constituents .....	19
4.4.2	Assessment of fuel quality .....	24
4.4.3	Evaluation of NIR-predicted mass flows.....	24
4.5	<i>Conclusion</i> .....	24
5	Effects of changing sky cover on hyperspectral reflectance measurements for dry matter yield and forage quality prediction.....	26
5.1	<i>Introduction</i> .....	27
5.2	<i>Material and methods</i> .....	29

5.2.1	Experimental design and reference data .....	29
5.2.2	Spectral data collection.....	30
5.2.3	Determination of darkening levels for simulating different degrees of sky cover and signature of the artificial illumination source.....	31
5.2.4	Analysis of spectral data .....	33
5.3	<i>Results and discussion</i> .....	35
5.3.1	Sward characteristics, DM yield and quality parameters .....	35
5.3.2	Spectral signatures in response to darkening levels and illumination.....	36
5.3.3	Relationships between prediction accuracy of dry matter yield, nutritive values and simulated sky cover with solar and artificial illumination.....	39
5.4	<i>Conclusions</i> .....	44
6	Off-nadir hyperspectral measurements in maize. Comparison of different angle-height combinations for on-the-go-solutions to predict DM yield, protein and ME contents in total biomass.....	46
6.1	<i>Introduction</i> .....	47
6.2	<i>Material and methods</i> .....	48
6.2.1	Experimental design and reference data .....	48
6.2.2	Spectral data collection.....	50
6.2.3	Spectra pre-processing.....	51
6.2.4	Calculation of Simple Ratio vegetation index and analysis of variance.....	51
6.2.5	Cross-Validation .....	51
6.3	<i>Results and discussion</i> .....	53
6.3.1	Canopy characteristics, DM yield and quality parameters .....	53
6.3.2	Dependency of reflectance on angle and height.....	55
6.3.3	Prediction of DM yield, CP and ME in total biomass as related to angle and height.....	56
6.3.4	Comparison of nadir and off-nadir measurements .....	58

6.4	<i>Conclusions</i> .....	62
7	General discussion .....	63
8	Conclusions.....	66
9	Summary.....	67
10	Zusammenfassung .....	69
11	References.....	71



## Tables

### Chapter 4:

Table 4.1: Number of reference samples, separated in calibration and validation set and their composition on a dry matter basis.....	16
Table 4.2: Correlation coefficients (r) among chemical parameters in samples.....	17
Table 4.3: Calibration and validation statistics for the constituents for press cakes including number of outliers and best math treatment.....	18
Table 4.4: Statistics for mass flows , based on measured values, and coefficient of determination (RSQ) of the relationship between measured and NIR-estimated mass flows from the parent material into the press fluid.....	19

### Chapter 5:

Table 5.1: Averaged growth stages and sward heights (cm) of red clover and Italian ryegrass and descriptive statistics of DM yield (t/ha), XP (%), ASH (%) and ME (MJ/(kg DM)).....	34
Table 5.2: Statistics of the cross-validation for DM yield (t/ha) for clear sky conditions and the overall calibrations with and without artificial light. The best scatter corrections and math treatments for the cross-validation, the standard errors of cross-validation (SECV), the coefficient of determination (RSQcal) of the cross validation and the stability factor RSC are given.....	40
Table 5.3: Statistics of the validation of DM yield (t/ha) for each darkening level, based on clear sky calibration models with and without artificial light. The standard error of prediction (SEP), the coefficient of determination (RSQval) of the linear regression and the stability factor RPD are given.....	41
Table 5.4: Statistics of the cross-validation for XP (%), ASH (%) and ME (MJ/(kg DM)) for overall calibrations with and without artificial light. The best scatter corrections and math treatments for the cross-validation, the standard errors of cross-validation (SECV), the	

coefficient of determination (RSQcal) of the cross validation and the stability factor RSC are given.....44

Chapter 6:

Table 6.1: Averaged growth stages and canopy heights (cm) of maize (*Zea mays* cv Ambrosius) and descriptive statistics of dry matter yield (DM) [t/ha], crude protein (CP) [% DM], and metabolisable energy (ME) [MJ/kg DM] .....54

Table 6.2: Effect of angle and height and the interaction angle x height on reflectance, expressed by the Simple Ratio (SR) vegetation index. ....56

Table 6.3: Statistics of the cross-validation (CV) for DM yield (DM) [t/ha], crude protein (CP) [% DM] and metabolisable energy (ME) [MJ/kg DM] of the total crop biomass. Shown are these height and angle combinations for which SECV was lowest in the entire (355 – 2300 nm) and reduced (620 – 1000 nm) wavelength range. ....57

Table 6.4: Calibration statistics of S1-scenario, when angle and height are adopted from the main target variable as determined in the S3-scenario for the entire (355 - 2300 nm) and reduced (620 - 1000 nm) wavelength range.....59

Table 6.5: Statistics of the cross-validation (CV) for DM yield (DM) [t/ha], crude protein (CP) [% DM] and metabolisable energy (ME) [MJ/kg DM] of nadir measurements for the entire (355- 2300 nm) and reduced (620 - 1000 nm) wavelength range and relative reduction in RSC with off-nadir measurements compared to nadir measurements. ....61

## Figures

### Chapter 3:

- Figure 3.1: The dominant factors controlling leaf reflectance of healthy, green vegetation for the wavelength interval 400-2600 nm (Source: Jensen, 2000). .....6
- Figure 3.2: Dependency of reflectance on sun/sensorview geometry (Source: Jensen, 2000). .....7

### Chapter 4:

- Figure 4.1: Flow chart of the IFBB (Integrated Generation of Solid Fuel and Biogas from Biomass) procedure. CHP refers to a combined heat and power plant. ....10
- Figure 4.2: NIR predicted versus reference values for CF, NFE, EE and ash.....20
- Figure 4.3: NIR predicted versus reference values for K, Cl, P and N.....22
- Figure 4.4: Press cakes (PC), beechwood (B), woodchips (willow and poplar; WC) and grains (wheat, rye and Triticale; G) compared with regard to major quality parameters for combustion chloride (Cl), potassium (K), nitrogen (N) and gross energy (GE).....23

### Chapter 5:

- Figure 5.1: Reduction of reflectance under four different darkening levels (R67 – R26) compared to the standard measurement (R100) (spectra are exempt from stray light effects and water band noise at 1400 nm). .....32
- Figure 5.2: Measured spectra of defined darkening levels (R67-R26) compared to clear sky conditions (R100). a) DOY 141, b) DOY 175 (white reference and measurements were conducted under the rack). .....37
- Figure 5.3: Measured spectra of defined darkening levels (R67-R0) compared to clear sky conditions (R100) using artificial illumination. a) DOY 141, b) DOY 175 (white reference and measurements were conducted under the rack). .....38
- Figure 5.4: Measured and predicted values of DM yield [t/ha] under clear sky conditions (R100) a) without artificial light, b) with artificial light

and under changing sky covers c) without artificial light and d) with artificial light. Lines indicate $y=x$ .....	42
Figure 5.5: Measured and predicted values of CP [%], ash [%] and ME [MJ/kg DM] under changing sky covers with (R100-R0) and without (R100-R26) artificial light. Lines indicate $y=x$ . ....	43
<u>Chapter 6:</u>	
Figure 6.1: Schematic measuring setup for nadir (a) and off-nadir (b+c) measurements, including sensor field of view (a+b); segment heights (b) and zenith view angle (c). ....	49
Figure 6.2: Mean segmental content of ME, CP and DM yield in maize plants for each measurement date in 2008. Plant material higher than 250 cm was included in segment height 200 – 250 cm for reference analysis.....	55
Figure 6.3: Relative reflectance depending on a) segment height and b) zenith view angle adjustments. Spectra are exempt from water absorption bands at 1400 nm and 1900 nm. ....	56

## Abbreviations

CF: crude fibre

CHP: Combined Heat and Power Plant

CP: crude protein

DM: dry matter

DOY: day of year

EE: ether extract

GE: gross energy

IFBB-System: **I**ntegrated **G**eneration of **S**olid **F**uel and **B**iogas from **B**iomass

ME: metabolizable energy

MF: mass flow

MPLS: modified partial least squares

MSC: multiplicative scatter correction

NDVI: normalized difference vegetation index

NFE: nitrogen free extracts

NIR: Near infrared reflectance

NIRS: near infrared spectroscopy

PMC: parent material after hydrothermal conditioning

r: coefficient of correlation

RPD, RSC: residual predictive value

$RSQ_{cal}$ ,  $R^2_{cal}$ ,  $R^2_{cv}$ : coefficient of determination of the cross validation

$RSQ_{val}$ : coefficient of determination of the validation

SD: standard deviation

SE: standard error

SEC: standard error of calibration

SECV: standard error of cross validation

SEP: standard error of prediction

SNV: standard normal variate

SR: simple ratio

VI: vegetation index



## 1 General introduction

In the context of the global increase of energy consumption, it is essential to develop sustainable energy supply systems (Amon *et al.*, 2007). Energy from biomass can make a significant contribution in order to mitigate green house gas emissions. Hereby, biogas production is one of the most important technologies for the sustainable use of agrarian biomass as renewable energy source due to the large variety of parent materials digestible in a fermenter. The energy efficiency would further be increased, using combined heat and power plants (CHP) by an integrated approach that comprises the provision of highly digestible fluids for the fermenter as well as solid fuels destined for combustion (Reulein *et al.*, 2007; Graß *et al.*, 2009; Richter *et al.*, 2009b). Maize, sunflower, rapeseed, grass and Sudan grass are the most commonly used energy crops (Wachendorf *et al.*, 2009). Furthermore, other sources of biomass, such as municipal biological wastes and residual material from forest, agriculture and nature conservation areas, might be adequate for digestion, since the cultivation of energy crops often competes with food production for limited agricultural land (Wachendorf *et al.*, 2009).

With the focus on bio-energy production rather than on forage provision, specifically required biophysical and biochemical parameters come to the fore (e.g. high methane yield per ha) which might result in different harvesting strategies, procession technologies and genotypes (Amon *et al.*, 2007). In addition it is of essential importance to implement sustainable and versatile crop rotations, as practised in organic agriculture, in order to reduce ecological impact and thus, to achieve lasting success. Hence, especially for organic agriculture, the provision of ecologically produced parent materials for a local energy production is of great importance.

The wide variety of crops potentially fed to a biogas plant requires a permanent quality management in order to guarantee high methane yields during the fermentation process. Since wet chemical analysis often is time, labour and cost intensive, other standardised laboratory methods such as near infrared reflectance spectroscopy (NIRS) show promising characteristics for an online quality management. NIRS only needs few sample preparation, and is generally characterised by

a fast, clean and reliable analysis of target parameters such as fibre, protein and ash contents (Stuth *et al.*, 2003). However, there would be advantages in further reduction of preparation efforts.

One strategy is to detect required target parameters on fresh plant material in the field using a non destructive sensor based approach. Remote sensing, normally supported by satellites, is verifiable suitable to detect variations in vegetation species and community distribution patterns, alterations in vegetation phenological cycles, and modifications in the plant physiology and morphology (Jensen, 2000). However, satellite based systems often show low spatial resolution and might not be suitable for crop specific quality management in a heterogeneous canopy. In contrast, the adaptation of NIRS to field conditions might be an adequate solution in order to measure quality features in spatially limited systems. Field spectroscopy offers the hyperspectral collection in a wide wavelength range covering visible, near infrared and short-wave infrared light (350 – 2500 nm) and hence, provides a large amount of plant physiological information.

The examination of the applicability of NIRS and field spectroscopy in the context of energy crop production and quality management takes centre stage of this thesis. Thereby the enhancement of (field)-spectroscopic measurements is of great importance and will be content of the following chapters.



## 2 Research objectives

The main objective of this study was to evaluate the potential of analysis methods based on light-pattern interaction to predict dry matter (DM) yield and nutritive values of crops for energetic purpose across a wide range of species.

In a first attempt a laboratory study was conducted using samples characterised by heterogeneous parent materials, partly containing high amounts of less-digestible fibre and ash. Subsequently, field spectral measurements of a binary legume-grass mixture and of maize were conducted to examine practical approaches in order to overcome known limitations of this technique.

The specific objectives of these investigations were:

- i) to explore the potential and accuracy of NIRS for examining quality properties of heterogeneous sets of press cakes from mechanically dehydrated silages and to assess mass flows of the **I**ntegrated Generation of Solid **F**uels and **B**iogas from **B**iomass (IFBB)-System,
- ii) to examine the influence of clouds on field spectroscopic measurements and the application of artificial light sources in order to compensate these impacts on the prediction accuracy of DM yield, ash, ME and CP by means of nadir measurements recording top-of-canopy reflectance and
- iii) to develop optimum reflectance algorithms for the prediction of DM yield and the forage quality constituents ME and CP in total biomass based on off-nadir reflectance measurements inside a canopy with heights of more than three meters.

### 3 Basic principles of spectroscopy

Incident optical radiation can be reflected, transmitted or absorbed by matter. Spectroscopy is a widely used method that measures light absorption/reflectance in order to predict quality and quantity parameters of materials.

The basic principle relies on an excitation of electrons or chemical bonds within molecules by discrete radiative energy quantities or wavelengths. These molecules are characterised by an asymmetric constitution of charge, resulting in permanent or induced dipoles and dipole moments, respectively. The outcomes of these processes are molecule vibrations or rotations and combinations of both, identifiable by peaks in a continuous spectrum at distinctive wavelengths. In laboratory NIRS devices this excitation is induced by an artificial light source whereas for field spectroscopic application in general the sun serves as lighting source. Near infrared spectroscopy primarily detects organic functional groups such as C-H, N-H, O-H, and C-O (Rudzik, 1993), whereas mineral composition and ions generally do not react with infrared light. Nevertheless, prediction of minerals is possible by detecting chelates and complexes, where minerals are bonded to.

#### 3.1 The Beer-Lambert Law

The quantitative determination of constituents is based on a linear correlation of absorbed radiance by the matter and the concentration of a distinct constituent. This relationship is described in the Beer-Lambert law, usually written as:

$$A = a(\lambda) * b * c, \quad (3.1)$$

where  $A$  is the measured absorbance,  $a(\lambda)$  the wavelength-dependent absorptivity coefficient,  $b$  the path length and  $c$  the concentration of the constituent.

The important feature of this relationship is the possibility of measuring the concentration of the constituent directly from the amount of absorbed irradiance. Each pure material has its own characteristic spectrum. However, the absorbance is assumed as cumulative. In a mixture this entails that the total radiative absorption equals the sum of absorptions of individual components. The resulting spec-

trum is characterised by many peaks at different wavelengths, partly overlapping each other and a direct measurement of concentrations is not possible anymore.

Furthermore, the linearity of the Beer-Lambert Law is limited by chemical and instrumental factors. Chemical limitations comprise deviations in absorptivity coefficients at high concentrations due to electrostatic interactions between molecules in close proximity, scattering of light due to particle structure in the material as well as fluorescence and phosphorescence (spontaneous and delayed release of energy respectively) of the material. Instrumental factors are non-monochromatic radiation and stray light (Miller, 2001). In these cases the relationship between the concentration of the constituent and measured absorption must be calculated by using empirical models. For the development of these models usually the whole concentration range of the constituent is needed (Günzler and Gremlich, 2003).

### **3.2 Specific spectral characteristics of green vegetation**

In the context of agrarian issues of research living plants/canopies and their interaction with the sun take centre stage of the investigations. Due to the intercellular structure of plant tissues, green vegetation has distinctive spectral characteristics (Figure 3.1). In the visible light region electronic processes are dominating. These processes involve absorption of photons with specific energy contents or wavelengths, respectively that causes an electron transfer from a lower energy state to an electron shell at a higher energy state (Clark, 1999). Chlorophyll *a* and *b* are the most important plant pigments absorbing blue and red light: chlorophyll *a* at wavelengths of 430 and 660 nm and chlorophyll *b* at wavelengths of 450 and 650 nm (Curran, 1983; Schilling, 2000). Other pigments such as carotenes, xanthophylls, anthocyanin and phycoerythrin are also present in the plant cells, but usually masked by the abundance of chlorophyll pigments. When a plant undergoes senescence in the fall or encounters stress, the chlorophyll pigment disappears, allowing the carotenes and other pigments to become dominant (Jensen, 2000). Depending on the plant species and the amount and nature of the occurring pigments, the absorption intensity in the visible light differs between 70% and 95% of the solar irradiation (Hildebrandt, 1996). Normally green light is more reflected, resulting in a typical reflection maximum at about 500 nm (Figure 3. 1).

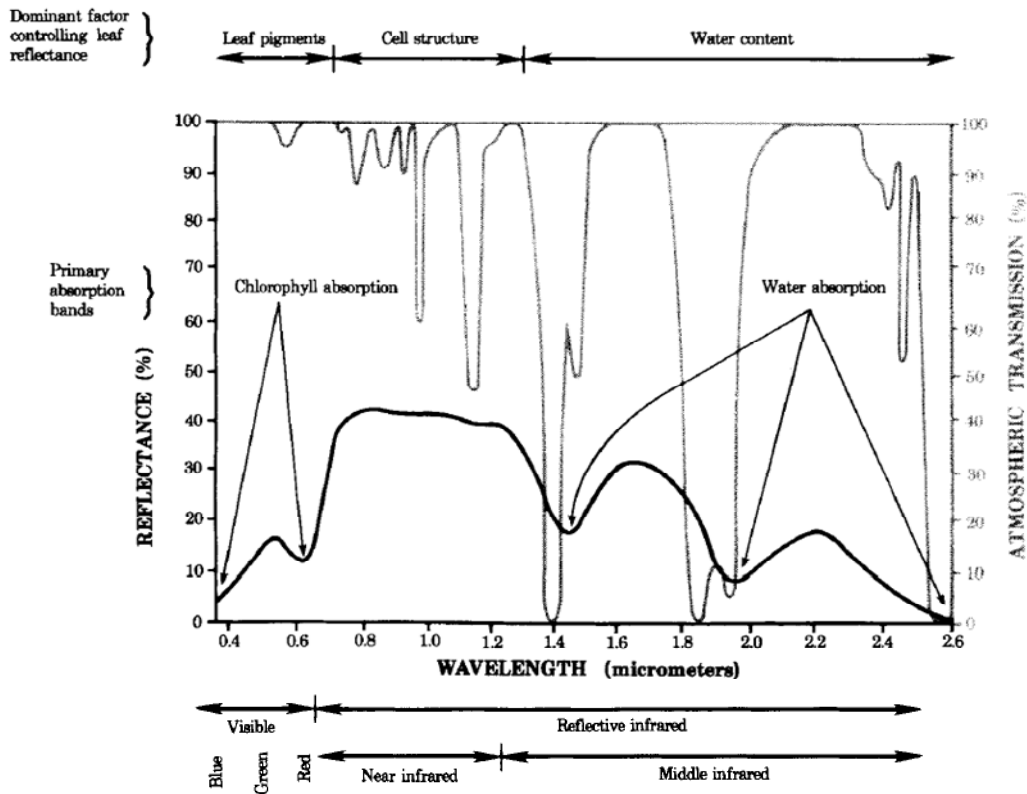


Figure 3.1: The dominant factors controlling leaf reflectance of healthy, green vegetation for the wavelength interval 400-2600 nm (Source: Jensen, 2000).

In the near infrared region, reflection and transmission processes on plant surfaces dominate. This prevents proteins from denaturation (Jensen, 2000). Thereby, the spongy mesophyll layer in a green leaf controls the amount of near infrared energy that is reflected by internal scattering at the cell wall-air interfaces within the leaf (Gausmann *et al.*, 1969). Especially water, present in the atmosphere and in the plant canopy, shows strong absorption features. Water in the atmosphere creates the four major absorption bands at 970, 1119, 1450 and 1940 nm (see Figure 3. 1). However, there is also a strong relationship between the irradiance and the amount of water present in the plant canopy. Water in plants absorbs incident energy between the absorption bands of atmospheric water with increasing strength at longer wavelengths. Reflectance peaks occur at about 1600 and 2200 nm (Jensen, 2000). The greater the turgidity of leaves, the lower is the reflection of near infrared light. Conversely, as the moisture content of leaves decreases, reflectance in the near infrared region increases substantially (Jensen, 2000).

Further plant constituents such as protein, carbohydrates, cellulose, lignin and fat, containing different functional groups, show broad absorption bands in the near infrared region.

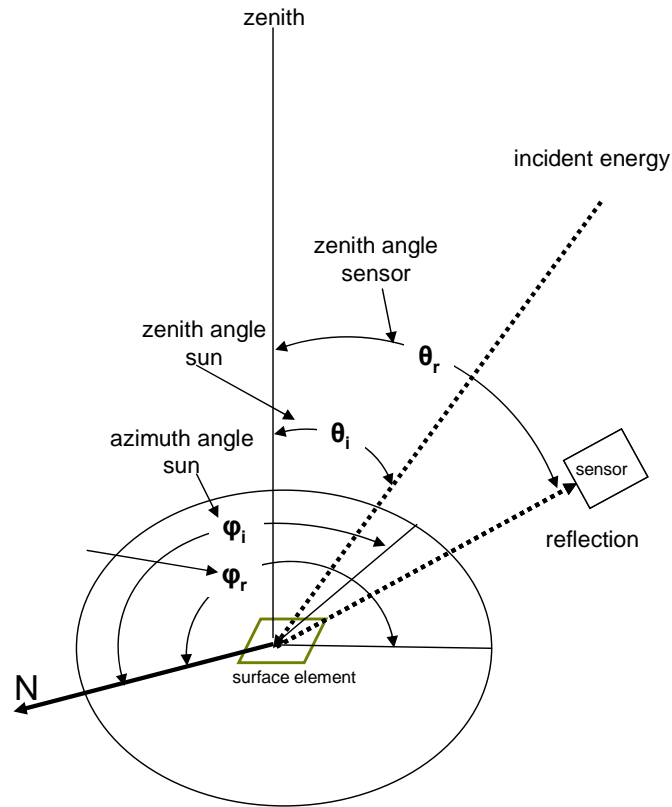


Figure 3.2: Dependency of reflectance on sun/sensor view geometry (Source: Jensen, 2000).

However, natural plant surfaces are characterised by a non-Lambertian reflectance behaviour, i.e., they reflect incident energy unequally, depending on solar incidence and azimuth angles as well as sensor viewing geometry (Jensen, 2000; Figure 3.2). Further variables, affecting recorded reflectance intensity are inter alia atmospheric turbidity, canopy type, leaf area index and leaf angle distribution as well as soil texture, colour and moisture content. All these vegetation factors have a significant impact on the reflection of radiation, and a constant, comprehensible measurement design is of great importance when attempting to extract biophysical or biochemical parameters (Jensen, 2000).

## 4 Assessment of mass flows and fuel quality during mechanical dehydration of silages using near infrared reflectance spectroscopy

**Abstract** This study was implemented to evaluate the potential of near-infrared reflectance spectroscopy (NIRS) technology to estimate chemical composition of dried press cake samples characterised by a wide range of parent materials. A total of 210 samples, derived from two studies on production of solid fuels from agricultural crops by application of the IFBB technology (Integrated production of solid fuels and biogas from biomass), were analysed to determine their chemical composition. A Foss XDS-spectrometer was used to obtain near-infrared spectra (400-2500 nm). Prediction equations, developed for chemical components, showed that NIRS technology could predict N, inorganic ash (ash), crude fibre (CF), ether extract (EE) and nitrogen free extracts (NFE) accurately (RSQ<sub>cal</sub> and SECV of 0.93 and 0.04 % DM, 0.89 and 0.48 % DM, 0.93 and 1.67 % DM, 0.87 and 0.28 % DM and 0.93 and 1.72 % DM, respectively). Mineral components could also be predicted with a moderate degree of accuracy using NIRS technology (RSQ<sub>cal</sub> and SECV of 0.85 and 0.10 % DM (K), 0.77 and 0.01 % DM (P) and 0.84 and 0.02 % DM (Cl), respectively), whereas calibration of gross energy (GE) did not succeed. Subsequent, external validation confirmed these results.

Regression of mass flows with measured and NIRS-predicted values showed accurate results (RSQ 0.72-0.99) and promise an accelerated quality management in working biogas plants.

**Keywords:** combustion; IFBB-system; mineral composition; NIRS; solid fuels

## 4.1 Introduction

Most common conversion techniques, i.e. anaerobic fermentation of silages or combustion of hay, straw and other herbaceous biofuels, have a limited conversion efficiency and face important technical limitations. In the case of biogas production, these are associated with the ligno-cellulose content of the biomass which is resistant to anaerobic fermentation and which inhibits digestion of readily fermentable compounds through their inclusion. Yields of methane decrease (Shiralipour and Smith, 1984; Amon *et al.*, 2007) and digestion times in the digester increase (Noike *et al.*, 1985; Lemmer and Oechsner, 2001) with decreasing digestibility of substrates. As a consequence, conversion efficiencies of biogas plants based on silages often are low (Prochnow *et al.*, 2005; Herrmann *et al.*, 2007). In order to achieve satisfactory conversion efficiencies waste heat from combined heat and power plants (CHP) must be used which accounts for 2/3 of the total energy contained in the biogas (Graß *et al.*, 2009). There is no exact data, but nearly all German biogas plants use the waste heat. It is estimated that the proportion varies between 5 and 100 % of the total heat available and on average less than 20 % of the total heat is used for heating or drying purposes in German biogas plants. A major problem in rural areas is that there is little demand for industrialised heat compared to urban areas.

As for combustion of arable crops, straw and hay, a major limitation lies in the increased dependency on weather conditions for achieving dry matter (DM) contents of 850 g/kg (Hartmann, 2001). Such DM contents are necessary to prevent microbial deterioration during storage. Compared to wood as the most common solid biofuel, herbaceous biomass contains more nitrogen (N), potassium (K) and chlorine (Cl). During combustion N is almost completely transformed into nitrogen oxides (NO<sub>x</sub>) which are major air pollutants (Greul, 1998). Potassium and Cl are significantly involved in corrosion processes in the furnace, and K promotes the melting of ash at low temperatures (Hartmann, 2001). While ash from wood melts at temperatures above 1200°C, ash from hay melts at temperatures below 1000°C (Hartmann, 2001). Melting of ash leads to slagging and fouling processes inside the combustion chamber, which reduces the efficiency of the processing plant and its life (Oberberger *et al.*, 2006).

### IFBB - Integrated Generation of Solid Fuel and Biogas from Biomass

With the aim of overcoming these problems, the Integrated Generation of Solid Fuel and Biogas from Biomass System was proposed (Wachendorf et al., 2009) which separates ensiled herbaceous biomass by a mechanical dehydration and results in a press liquid rich in easily degradable organic matter and a press solid consisting mainly of fibrous plant parts (Figure 4.1). The first step is a hydrothermal conditioning in which silage is mixed with water or other mash fluids (e.g. press fluid) and heated for a short time to macerate cell walls. This treatment produces a mash which is then mechanically dehydrated by a screw press. As an effect of conditioning and dehydration, several minerals (e.g. K, Mg and Cl) and organic compounds (e.g. water soluble carbohydrates, proteins and lipids) are transferred into the press fluid.

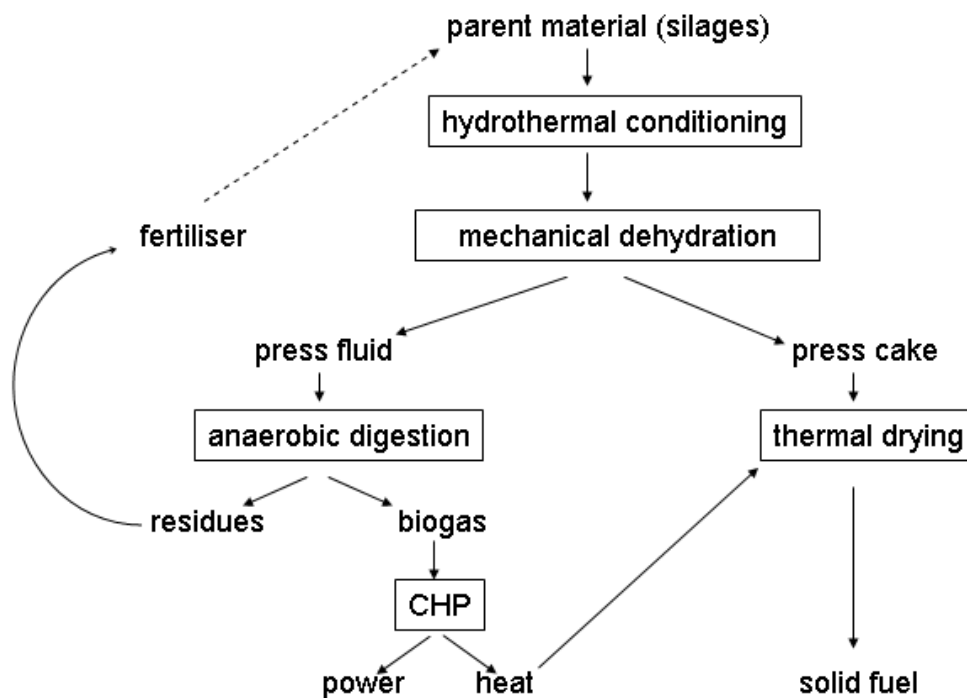


Figure 4.1: Flow chart of the IFBB (Integrated Generation of Solid Fuel and Biogas from Biomass) procedure. CHP refers to a combined heat and power plant.

Data from dehydration of whole-crop silages of maize, wheat and semi-natural grassland show that press fluids make an excellent substrate for anaerobic digestion with methane yields of up to 500 normal litre (NL)  $\text{CH}_4$   $\text{kg}^{-1}$  volatile solids and almost total degradation of organic matter in less than 15 days (Richter *et al.*,



2009; Graß *et al.*, 2009). Digester residue is an excellent liquid fertiliser with high concentrations of readily available nutrients. The biogas plant is easily charged and discharged and no stirring of digester fluid is necessary. The remaining press cake is rich in fibrous constituents and contains relatively low proportions of detrimental minerals, which increase the quality of the resulting biofuel (Wachendorf *et al.*, 2009; Graß *et al.*, 2009). With the need to dry the press cake from about 450-500 g/kg to 850 g/kg DM, the IFBB technology provides a year-round demand for heat produced in the CHP (Wachendorf *et al.*, 2009). For arable crops, Graß *et al.* (2009) calculated that approximately 50 % to 60 % of the gross energy contained in the crop is converted to electricity and heat (which is stored in the solid fuel). For semi-natural grassland, with a delayed cut and crude fibre contents well beyond 25 % of DM, conversion efficiencies were in the same range (Wachendorf *et al.*, 2009).

### **Focus of this study**

For technical application it is important to evaluate the process in all stages in time. For example, estimation of mass flows allows the calculation of the amount of nutrients to be recycled to the field, as well as the quantification of methane production from anaerobic digestion. This in turn allows estimation of the amount of heat from the combustion of biogas in the CHP, which is used for thermal drying of the press cake from approximately 40% to 85% of DM (Wachendorf *et al.*, 2009). On the other hand, value of solid biofuels for combustion depends primarily on the gross energy value and on concentration of nitrogen and minerals detrimental to combustion. However, wet chemical analysis is expensive and time intensive. A widely used and promising technique in agricultural quality management is near-infrared spectroscopy (NIRS) (Norris, *et al.*, 1976; Stuth *et al.*, 2003). It is well known that total nitrogen (N), inorganic ash (ash), crude fibre (CF), ether extract (EE) and nitrogen free extracts (NFE) can be determined with NIRS (e.g. Park *et al.*, 1998; Valdés *et al.*, 2006) as well as mineral compositions (Ruano-Ramos *et al.*, 1999a; Petisco *et al.*, 2005; González-Martín *et al.*, 2007). However, most studies concentrate on pure sample sets of wheat (Morón *et al.*, 2007), maize silage (Deaville *et al.*, 1998; Lovett *et al.*, 2004), herbages and grass silages (Nousiainen *et al.*, 2004; Andrés *et al.*, 2005), legumes (Halgersson *et al.*,

2004; Cozzolino *et al.*, 2004), rice (Wu *et al.*, 2002) sunflower (Moschner and Biskupek-Korell, 2006) or hemp (Toonen *et al.* 2004). Reliability of NIRS had been questioned when analysis was performed across different plant species and cultivars (Foley *et al.*, 1998; Ruano-Ramos *et al.*, 1999b). Moreover, there is a lack of knowledge of how much the dehydration and removal of easily mobilized organic and mineral constituents alters the spectral signature of biomass, affecting the relationship between NIR spectra and concentration of various constituents. The present study aims to develop a cheap and fast procedure to evaluate the potential of an energetic conversion of herbaceous crops with the IFBB technique. This includes

- exploration of the potential and accuracy of NIRS for examining quality properties of a heterogeneous set of press cakes from mechanically dehydrated silages, focusing on concentration of major constituents relevant for combustion
- assessment of mass flows of major organic and mineral constituents during mechanical separation, based on NIR-predicted values.

## 4.2 Material and Methods

### 4.2.1 Samples

A total of 210 press cakes from mechanically dehydrated silages were available for calibration. 187 samples derived from four experiments on arable land in Northern Germany. The samples were harvested from 2002 to 2004, chopped and ensiled in 60 l gas-proof polyethylene containers for a minimum of 28 days. In order to enhance the discharging of detrimental constituents 147 silages were conditioned prior to mechanical dehydration with different fluids (i.e. water, press fluid, digester fluid) of different temperatures (5°C, 60°C, 80°C, and 100°C, respectively) in a modified concrete mixer with a volume of 200 L, resulting in a mash with a silage:liquid ratios between 1:1 and 1:6. The mash was kept at a constant temperature with gas burners and stirred for 15 min in order to thoroughly rinse the silage with water. Dehydration of the silages was carried out using a screw press (type Av; anhydro Ltd., Kassel, Germany). Pressing was conducted with a conical pressing screw and a screen perforation of 1.5 mm in diameter. The

screw was at a pitch of 1:7.5 and rotated with 12 revolutions per minute. Press cakes were composed of the following species: maize (*Zea mays*), winter wheat (*Triticum aestivum*), canola (*Brassica napus*), winter rye (*Secale cereale*) and winter pea (*Pisum sativum*), as well as mixed silages of maize/sunflower (*Helianthus*), maize/barley straw (*Hordeum vulgare*), wheat/barley straw, winter pea/rye and winter vetch (*Vicia villosa*) (Reulein *et al.*, 2007). Twenty three press cakes derived from semi-natural grassland sites in Central and Southern Germany, representing typical European montane areas with two different poor oat-grass meadows (Arrhenaterion), a small sedge poor-fen meadow (Caricion fuscae), a tall herb vegetation meadow (Filipendulion ulmariae) and a montane hay meadow (Polygonum-Tristion). Due to the late harvest date in mid August, most species had finished flowering. The material was collected in 2006, conditioned with water (silage:liquid ratio 1:4) and mechanically dehydrated with the same screw press, described above. Details of the experimental setup can be found elsewhere (Wachendorf *et al.*, 2009).

#### 4.2.2 Reference analysis

Press cakes were dried at 60°C for a minimum of three days. Subsequently, N (calculated by CP/6.25), ash, CF, EE and NFE as well as potassium (K), chlorine (Cl) and phosphorus (P) were determined according to Naumann and Bassler (2004). In this study, we refer to N rather than CP due to the importance of nitrogen as an air pollutant in combustion processes.

Gross energy values (GE) were calculated for each press cake according to (GfE, 1995):

$$\text{GE [kJ/kg]} = 23.9 \cdot \text{CP [g/kg]} + 39.8 \cdot \text{EE [g/kg]} + 20.1 \cdot \text{CF [g/kg]} + 17.5 \cdot \text{NFE [g/kg]} \quad (4.1)$$

#### 4.2.3 Mass flow calculations

Assessment of mass flow values for specific chemical constituents is essential to evaluate the conditioning and dewatering procedure, as well as to calculate methane yields and corresponding heat from anaerobic fermentation of press fluids, and hence, to evaluate the IFBB-System. Mass flow (MF) of the constituents N,

ash, CF, EE, NFE, K, Cl and P (represented by Z; g/kg DM) from the parent material (PM) into the press fluid (PF) and the press cake (PC) were determined according to:

$$MF_{-Z_{PF}} = \frac{X \cdot DM_{PF} \cdot Z_{PF}}{DM_{PMC} \cdot Z_{PMC}} \quad (4.2)$$

$$MF_{-Z_{PC}} = 1 - MF_{-Z_{PF}} \quad (4.3)$$

where X is the quantity of the press fluid as a proportion of the parent material after hydrothermal conditioning (PMC), and  $DM_{PF}$  and  $DM_{PMC}$  are the amounts of dry matter in the press fluid and parent material after hydrothermal conditioning, respectively. A comprehensive derivation of these equations is given in Wachendorf et al. (2009).

#### 4.2.4 NIRS measurement

Reflectance spectra of the ground press cake samples (1 mm sieve, cyclotec® sample mill, Foss Tecator AB, Höganäs, Sweden) were obtained using a XDS-spectrometer (Foss NIRSystems, Hillerød, Denmark). Spectra were collected in the visible and near infrared range from 400 to 2500 nm with data collection every 2 nm. Each sample was scanned once using a small ring cup, which is a 45 mm circular capsule with a quartz window. The spectrum of each sample was an average of 25 sub-scans and was recorded as the logarithm of the inverse of the reflectance ( $\log(1/R)$ ). Data analysis was conducted using the WinISI software (version 1.63, Foss NIRSystems/Tecator Infrasoft International, LLC, Silver Spring, MD, USA). Spectral data were reduced by keeping the first of every eight consecutive spectral points (Azzouz *et al.*, 2003), resulting in 259 data points per spectra.

#### 4.2.5 Spectra pre-processing

To correct for differences in particle size and in the spectral curvature of the samples standard normal variate and de-trend scatter correction (SNV-D) (Barnes *et al.*, 1989) was performed. Mathematical pre-processing also included 1, 4, 4 and 2, 4, 4 treatments (number of derivative, wavelength gap over which the derivative is calculated and number of data points in a running average smooth, respec-

tively). Derivatives were used to reduce baseline variation and to enhance spectral features (Reeves *et al.*, 2002).

#### 4.2.6 Calibration

Modified partial least squares (Martens and Naes., 1989) (MPLS) method was used to develop calibration equations. Prior to analysis samples were divided into a calibration and a validation subset, where the validation set included 30 % of the total samples randomly chosen for each constituent (Cozzolino *et al.*, 2004; Brunet *et al.*, 2007) (Table 4.1). Calibration was done with the remaining samples. Full cross validation was performed on the calibration set. Therefore the calibration set was divided into five and six groups, respectively, depending on the amount of calibration samples. One group was used for predicting while the rest were available for developing the model. The procedure was performed until all samples were used for both model development and prediction. The number of factors giving the lowest final SECV determined the optimal number of terms to be used for the calibration and hence avoided an overfitting due to too many factors (González-Martín *et al.*, 2007), which reduces the validation performance. Two outlier elimination passes were conducted, removing T outliers ( $T > 2.5$ ), characterized by a large difference between reference and predicted values, and H outliers ( $H > 10$ ), i.e. samples whose spectra differed notably from the mean sample spectrum. Number of outliers was lowest for K with 3 and highest for EE, where 11 samples were eliminated (Table 4.3). Accuracy of calibration models was assessed based on standard error of cross validation (SECV) and coefficient of determination for cross validation ( $RSQ_{cal}$ ). The best equations, defined by lowest SECV, were used for validation. The above described spectral treatments and calibration techniques were chosen since they are known to give most accurate predictions of a wide range of parameters of dried samples (Nousiainen *et al.*, 2004).

Table 4.1: Number of reference samples, separated in calibration and validation set and their composition on a dry matter basis

Constituent	N <sup>°</sup>	EE <sup>°</sup>	ash <sup>°</sup>	CF <sup>°</sup>	NFE <sup>°</sup>	K <sup>°</sup>	P <sup>°</sup>	Cl <sup>°</sup>	GE <sup>#</sup>
Number of reference samples	187	209	187	159	122	177	107	177	121
Number of samples for calibration	131	146	131	110	85	125	76	124	83
Number of samples for validation	56	63	56	49	37	52	31	53	38
minimum	0.61	1.00	1.61	20.27	2.59	0.06	0.04	0.01	18068
maximum	1.89	17.40	25.49	66.48	66.84	7.35	0.54	0.96	21890
mean	1.96	2.73	4.61	35.01	52.06	0.60	0.08	0.13	18773
SD	0.15	1.60	2.32	6.97	8.31	0.58	0.05	0.09	387

<sup>°</sup>: Min, max, mean and SD in % DM; <sup>#</sup>: Min, max, mean and SD in kJ/kg TM

The same calibration procedure was conducted with the parent material in order to achieve NIR-estimated values for the mass flow calculations, resulting in an averaged  $RSQ_{cal}$  of 0.90 for all constituents.

#### 4.2.7 Validation

Prediction accuracy of models was evaluated on the validation subset, using validation  $RSQ_{val}$ , slope (a) and residual predictive value (RPD). Residual predictive value was defined as the ratio of standard deviation of the laboratory results to the standard error of prediction of the independent validation set and demonstrated how well the calibration models performed in predicting the independent reference data (Morón *et al.*, 2007). A RPD value greater than three was considered good and a RPD value in the range from 2.5 to 3 was still satisfying for analytical purposes in most of the NIR applications for agricultural products (Cozzolino *et al.*, 2006).

### 4.3 Results

NIRS calibration equations were developed for all constituents of the press cakes. Variability in chemical composition due to heterogeneous parent material was considered suitable to develop NIR calibrations (Table 4.1). Correlation between constituents was found to be highest for CF and NFE ( $r = -0.93$ ) (Table 4.2). Cor-

relation coefficients for some mineral constituents, comprising ash, K, Cl and NFE were in the range of -0.55 (Cl:NFE) and 0.83 (Cl:K).

Table 4.2: Correlation coefficients (r) among chemical parameters in samples

	ash	EE	CF	NFE	K	P	Cl
EE	0.03 <sup>ns</sup>						
CF	0.47***	-0.33***					
NFE	-0.71***	0.04 <sup>ns</sup>	-0.93***				
K	0.79***	0.10 <sup>ns</sup>	0.40***	-0.62***			
P	0.42***	0.00 <sup>ns</sup>	0.22 <sup>ns</sup>	-0.31*	0.37***		
Cl	0.73***	0.07 <sup>ns</sup>	0.30***	-0.55***	0.83***	0.43***	
N	0.16*	0.25***	-0.47***	0.22*	0.21**	0.08 <sup>ns</sup>	0.31*

significance level: ns: not significant, \*: 0.05; \*\*: 0.01; \*\*\*: 0.001

For N, EE, ash, CF, and NFE very good calibration results were produced by NIRS (Table 4.3), with coefficients of determination of the cross validation ( $RSQ_{cal}$ ) of 0.87 for EE, 0.89 for ash and 0.93 for CF, NFE and N. Standard errors of cross validation (SECV; % of DM) were low in relation to the range within the population. Selected math treatments were 2,4,4 for N, ash and CF and 1,4,4 for EE and NFE. Subsequent validation with an independent sample set confirmed the good calibration results with  $RSQ_{val}$  in the range of 0.90 for NFE and 0.95 for ash and slopes between 0.88 (ash) to 1.02 (NFE). All constituents showed high RPD values, affirming the robustness of calibration equations (Table 4.3, Figure 4.2).

Calibration results of K, P and Cl were moderate with low SECV as well as fairly high  $RSQ_{cal}$  (Table 4.3). Best equations were achieved with math treatments 1,4,4 for P and 2,4,4 for K and Cl. Potassium also showed good validation results with  $RSQ_{val}$  of 0.93, slope of 0.89 and RPD of 3.9. In contrast, P and Cl attained poorer validation results with lower  $RSQ_{val}$  (0.81 and 0.79, respectively) and RPD (2.2 for both) (Table 4.3, Figure 4.3), which suggest a lack of robustness of these calibration equations.

Calibration of gross energy (MJ/kgDM), which is an important parameter describing the energy content of solid fuels resulted in  $RSQ_{cal}$  of 0.77 and  $RSQ_{val}$  of 0.39 (results not shown) and thus did not reach adequate accuracy of prediction.

Table 4.3: Calibration and validation statistics for the constituents for press cakes including number of outliers and best math treatment

Constituent	Calibration				Validation			
	Outliers removed	SD	SECV (% DM)	RSQ <sub>cal</sub>	Math Treatment	SEP (% DM)	RSQ <sub>val</sub>	RPD
N	7	0.16	0.04	0.93	244	0.04	0.90	3.7
EE	11	0.78	0.28	0.87	144	0.26	0.91	3.0
ash	6	1.51	0.48	0.89	244	0.43	0.95	4.4
CF	7	6.53	1.67	0.93	244	1.61	0.94	3.8
NFE	9	6.75	1.72	0.93	144	1.28	0.97	5.6
K	3	0.27	0.10	0.85	244	0.07	0.93	4.0
P	6	0.02	0.01	0.77	144	0.01	0.81	2.2
Cl	8	0.06	0.02	0.84	244	0.03	0.79	2.2

SD: standard deviation; SECV: standard error of cross validation; RSQ<sub>cal</sub>: coefficient of determination of the cross validation; math treatment: the first number is the order of the derivative function, the second number is the segment length in data points over which the derivative was taken, the third is the segment length over which the function is smoothed; SEP: standard error of prediction; RSQ<sub>val</sub>: coefficient of determination of the independent validation; RPD: ratio of SD and SEP.

A central parameter for evaluating the IFBB procedure is the mass flow of organic and mineral constituents into the press fluid and press cake. Two data sets of mass flows were calculated, one based on laboratory data and one obtained by NIRS estimated values. Subsequently, a regression was conducted with both data sets to evaluate the prediction accuracy of mass flows in an automated quality management. The mineral group (K, Cl and P), ash and GE show narrow ranges for mass flows from parent material into press fluid with a minimum value of 13 % for GE, and a maximum of 95 % for Cl and K, respectively (Table 4.4). CF, EE and NFE show broad ranges of mass flows with minima between 3 % (EE) and 13 % (NFE) and maxima between 68 % (CF) and 83 % (NFE). The regression resulted in very good prediction accuracies for all constituents (RSQ from 0.89 to 0.99), except of Cl which shows a somewhat lower accuracy with an RSQ value of 0.72 (Table 4.4).



Table 4.4: Statistics for mass flows, based on measured values, and coefficient of determination (RSQ) of the relationship between measured and NIR-estimated mass flows from the parent material into the press fluid.

constituent	n	min (%)	max (%)	mean (%)	RSQ
N	26	22	68	52	0.94
ash	28	32	87	51	0.89
CF	18	5	68	23	0.97
EE	28	3	83	31	0.92
NFE	20	13	82	34	0.98
Cl	23	32	95	64	0.72
K	19	33	95	72	0.91
P	10	44	85	67	0.97
GE	23	13	49	27	0.99

n: number of samples used for regression, min: minimum, max: maximum

Although GE could not be predicted well by NIRS both for parent material and press cakes, a close relationship existed between measured and calculated GE mass flows based on good calibration results for organic constituents used for calculation of GE.

## 4.4 Discussion

### 4.4.1 Prediction accuracy for solid fuel constituents

High correlations among the constituents found in this study were in line with other studies (DeBoever *et al.*, 1996; Park *et al.*, 1998) and were ascribed to the interrelation of lignin, hemicellulose and cellulose during the analytical extraction process and minerals which were chelated, or closely bound to organic compounds.

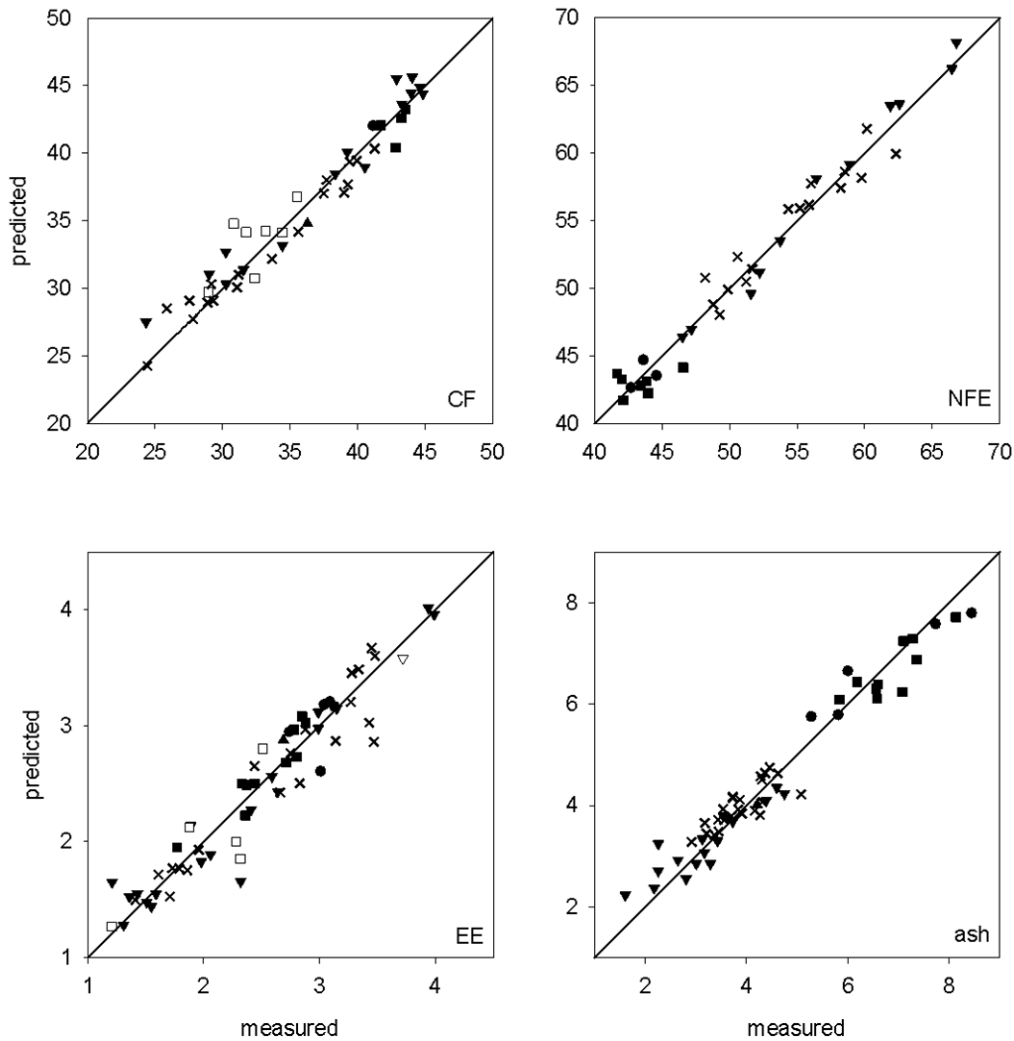


Figure 4.2: NIR predicted versus reference values for CF, NFE, EE and ash (▼ = maize; × = maize+ straw; ▲ = maize+sunflower; ▽ = vetch+rye; ● = wheat; ■ = wheat+straw; ○ = rapeseed; □ = grassland) Lines indicate 1:1

The calibration results for all constituents were similar to former studies dealing with dried samples of various crops, usually without ensiling or any pre-treatment. Cozzolino *et al.* (2006) reported  $RSQ_{cal}$  of 0.91 and a RPD factor of 4.8 for the prediction of N, whereas Valdés *et al.* (2006) and Morón *et al.* (2007) obtained better RSQ values (0.97) and RPD factors (3.9 and 8.5, respectively). For the prediction of crude lipid Berado *et al.* (1997) found satisfying results in dried pigeon peas with SEC of 2.5 and RSQ of 0.97, whereas DeBoever *et al.* (1996) reported poor calibration results in grass silages (accounted variance of 57.3 %, SEP of 5 g/kg and SD/SEP of 1.5). The authors ascribe their poor results to systematic errors arising from different residual moisture contents and a small number of cali-

bration samples as well as to the heterogeneous nature of crude lipid in grass silages. The same study obtained good results for ash, as did Park *et al.* (1998), who had similar results with a coefficient of determination of the cross validation ( $R^2_{cv}$ ) of 0.87 and SD/SECV of 2.83. The results for crude fibre in the present study are comparable with results achieved by DeBoever *et al.* (1996, 1997) in grass and maize silages. In contrast, Xiccato *et al.* (2003) reported poor prediction accuracy of crude fibre with  $R^2$  of 0.60 and SEP of 16 g/kg. The results for nitrogen free extracts (NFE) were similar to those reported by Castrillo *et al.* (2005) but showed, regarding the RPD values, a markedly higher robustness.

Ruano-Ramos *et al.* (1999a) achieved slightly better results regarding K and P for sample sets of semi-arid grasslands with a  $R^2$  of 0.92 and 0.88 as well as a SEC of 1.76 and 0.22, respectively, using log 1/R calibrations. Halgerson *et al.* (2004) investigated alfalfa stems and leaves and achieved better results for K ( $R^2$  of 0.95; SEC of 1090) in oven-dried alfalfa stems and for P ( $R^2$  of 0.91; SEC of 150) in sun-cured alfalfa leaves. The examination of ground alfalfa samples yielded in a  $R^2$  of 0.89 (SEC of 1180) and 0.90 (SEC of 244) for K and P, respectively, as reported by González-Martín *et al.* (2007). Residual predictive value (RPD) factors reported by the same authors were similar to those achieved in the present study for K (3.4) but much better for P (3.6). However, low accuracies of P estimation were found by Petisco *et al.* (2005) using an external validation set and RPD factors.

Only one study could be found reporting calibration results for chlorine in oven dried alfalfa stems (Halgerson *et al.*, 2004) with a coefficient of determination of the cross validation ( $R^2_{cv}$ ) of 0.84, which are in line with our results. However, the validation with independent samples of press cakes showed a lack of accuracy for Cl estimation. These results may be related to the difficulty of estimating mineral concentrations by NIRS. Cozzolino and Morón (2004) quoted that SEC and  $R^2_{cal}$

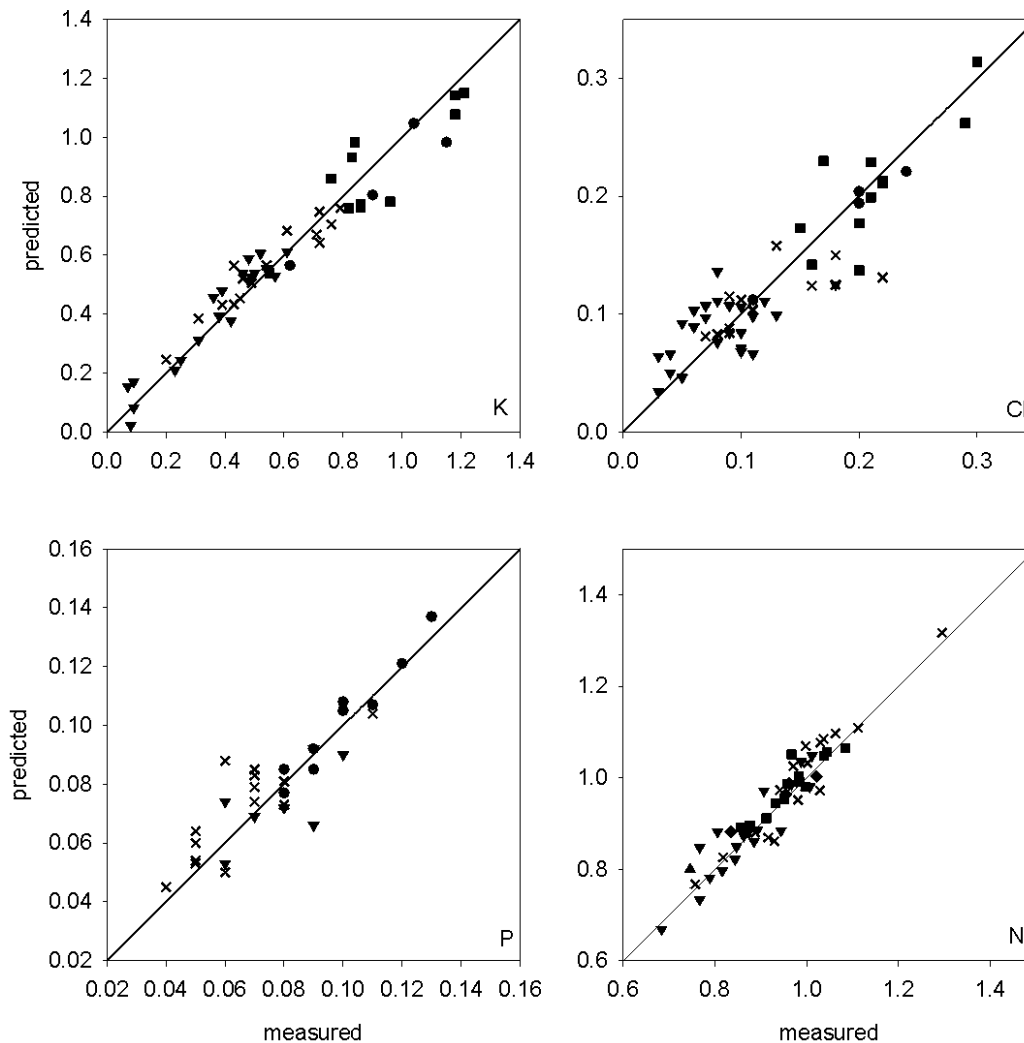


Figure 4.3: NIR predicted versus reference values for K, Cl, P and N ( $\nabla$  = maize;  $\times$  = maize+straw;  $\blacktriangle$  = maize+sunflower;  $\nabla$  = vech+rye;  $\bullet$  = wheat;  $\blacksquare$  = wheat+straw;  $\circ$  = rapeseed;  $\square$  = grassland). Lines indicate 1:1

were inappropriate indicators for mineral determination, because the NIRS was not directly measuring the element, but the organic compound the element was related to (Park *et al.*, 1998; González-Martín *et al.*, 2007) or through its association with hydrated inorganic molecules. According to Cozzolino and Morón (2004),  $R^2$  values in mineral determination are governed more by the amount or variability (range in concentration) present than by a direct relationship between variation in concentration and absorption in the NIR region.

Reasons for the low prediction accuracy of GE may be the narrow range of values (Table 4.1) which is in line with data from previous experiments (Stülpnagel *et al.*, 2008) as well as the error inherent to the regression equation used to calculate

gross energy (see equation 4.1). Furthermore, unlike energy values used in feed evaluation systems (e.g. net energy lactation, NEL) which are strongly related to

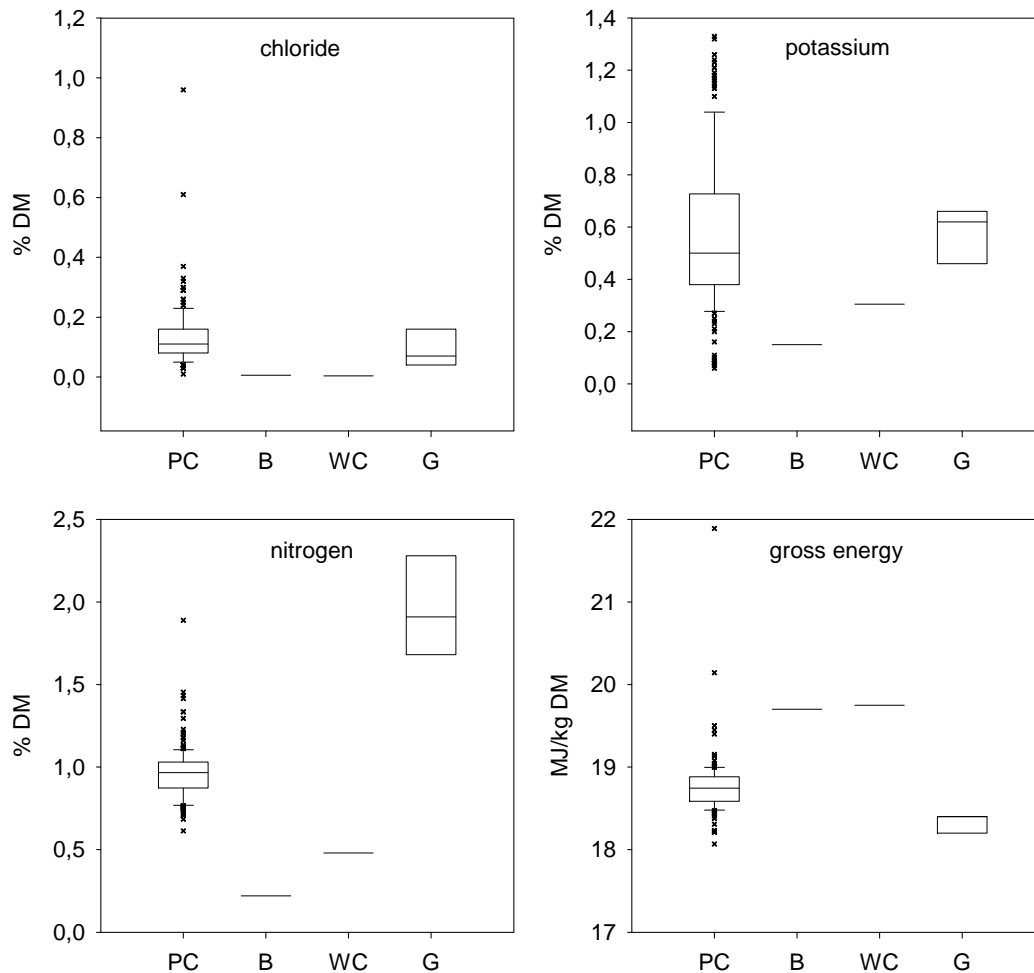


Figure 4.4: Press cakes (PC), beechwood (B), woodchips (willow and poplar; WC) and grains (wheat, rye and Triticale; G) compared with regard to major quality parameters for combustion chloride (Cl), potassium (K), nitrogen (N) and gross energy (GE)

fibrous constituents and usually well-predicted by NIRS (Volkers *et al.* 2003) gross energy is a complex parameter which is affected by all organic constituents of the fuel. Thus, albeit prediction accuracy by NIRS was unsatisfactory the calculated gross energy values may be plausible, which is suggested by the conformity with calorimetric data from various crops in a previous study (Stülpnagel *et al.*, 1992).

#### 4.4.2 Assessment of fuel quality

To evaluate the combustion quality of press cakes from herbaceous crops quality values of press cakes were compared with those from common solid biofuels i.e. beechwood, woodchips (willow and poplar) and grains (wheat, rye and triticale) (Hartmann, 2001), regarding four major constituents (N, K, Cl and GE) (Figure 4.4). Although the press cake data show a broad variation, a comparable or better quality than grains, especially for N and GE, was achieved. However, quality of press cakes was generally inferior to wooden biomasses, indicating the need to adapt the combustion appliance to inferior feedstocks.

#### 4.4.3 Evaluation of NIR-predicted mass flows

The high prediction accuracy for mass flows of organic and mineral constituents in the IFBB procedure is an important outcome of the present study, as it provides a basis for a cheap and accelerated assessment of the operating status of a continuously working plant. However, the presented NIRS procedure depends on dried and ground material both from parent material and press cake, which prolongs the system response time. The use of field spectroscopy may provide perspectives for a further acceleration as recent calibration work showed promising results for major quality parameters of various forage crops (Biewer *et al.*, 2009c).

### 4.5 Conclusion

The NIRS technology has good potential for evaluation of the IFBB process, as it establishes the basis for a cheap and fast assessment of several important parameters in the energetic conversion of herbaceous crops. The results of the present study with a heterogeneous set of press cakes from mechanically dehydrated silages of herbaceous crops show that,

- the concentration of major constituents relevant for combustion can be predicted with satisfactory accuracy. Lowest validation errors were achieved with SEP of 0.01 % DM for P, while SEP of CF was highest with 1.61 % DM. Fuel quality of press cakes obtained in the study was higher than that from cereal grains, but lower than that from wooden biomasses.

- mass flows of major organic and mineral constituents during mechanical separation based on NIR-predicted values can be assessed with appropriate accuracy (RSQ 0.72 – 0.99). These parameters are major determinants of the operating status and constitute a prerequisite for an effective system control.

## 5 Effects of changing sky cover on hyperspectral reflectance measurements for dry matter yield and forage quality prediction

**Abstract** Sensor based analysis methods to assess dry matter yield and nutritive values of legume-grass swards are time and labour saving and can facilitate a site-specific forage management. Nevertheless, in-field measurements, based on canopy reflectance are highly dependent on weather conditions, like e.g. wind or clouds. This study was conducted to explore the potential of field spectral measurements for a non destructive prediction of dry matter yield (DM), metabolisable energy (ME), ash content (ash), and crude ash (CP), of a binary legume-grass mixture (*Trifolium pratense* L. and *Lolium multiflorum* L.) under changing weather conditions. Five different degrees of sky cover were simulated by shadowing measurement plots with layers out of cotton to reduce incoming radiation at different growth stages (leaf developing to flowering). Additionally, a halogen lamp was established over the plots to examine the influence of an artificial light source on the spectral response under changing cloud stages. Modified partial least squares (MPLS) regression was used for analysis of the hyperspectral data set (350-2500 nm). Artificial illumination led to spectral interferences of solar radiation and additional light, and hence, partly reduced prediction accuracies. In contrast, prediction accuracy increased, when solar radiation was completely excluded. Results show good to very good prediction accuracies for DM yield and nutritive values, if the data basis covers all possible degrees of sky cover and instrument calibration and target measurement is carried out under the same illumination conditions.

**Keywords:** grassland, biomass yield, forage quality, field spectroscopy



## 5.1 Introduction

The application of remote sensing for estimating biophysical and biochemical parameters of forage swards is increasingly seen as an important first step in providing detailed and accurate information on their spatial and temporal variability. In this context, cultivated grassland has been the subject of numerous studies that have demonstrated a consistent functional relationship between agronomical canopy attributes such as biomass yield (Schino *et al.*, 2003; Numata *et al.*, 2007; Biewer *et al.*, 2009b) or LAI (Friedl *et al.*, 1994; Griffith *et al.*, 2001) and spectral response. Most of the studies for quantifying biochemical and biophysical parameters by remote sensing derived their data from satellite based broadband sensors such as SPOT and Landsat TM/ETM+ with only few spectral bands (Walter-Shea *et al.*, 1997; Price *et al.*, 2002; Wylie *et al.*, 2002; Daughtry *et al.*, 2006) and focused on developing empirical relationships between ground-measured vegetation parameters and calculated vegetation indices (VIs). However, there are major limitations with VIs despite their wide application in agronomical remote sensing. Several studies show that vegetation indices can be unstable, varying with soil colour, canopy structure, leaf optical properties and atmospheric conditions (Qi *et al.*, 1995, Todd *et al.*, 1998, Biewer *et al.*, 2009b). In contrast, most hyperspectral sensors record radiance information in less than 10 nm bandwidths from the visible (400-700 nm) to the short wave infrared (SWIR; 700-2500 nm) (e.g., Asner *et al.*, 1998, Lee *et al.*, 2004; Rees *et al.*, 2004; Starks *et al.*, 2008). Recent applications of hyperspectral remote sensing show improvements in the estimation of canopy parameters by including the whole spectral range (Broge and Leblanc, 2000; Bannari *et al.*, 2006; Xavier *et al.*, 2006; Govender *et al.*, 2008). However, it is common knowledge that all remote sensing methods are highly dependent on atmospheric turbidity, since clouds determine the solar radiation received at the ground in a most decisive way (Reusch, 1997; Zangvil and Lamb, 1997). With clouds covering the sky the fraction of scattering light increases and the fraction of direct radiance decreases (Wörner, 1972; Reusch, 1997). Furthermore, depending on optical depth, shape and spatial distribution of clouds over the sky in relation to the sun's apparent position, scattering and absorption by cloud particles can have different effects on the sky radiance and on diffuse irradiance (Feister

and Shields, 2005; Schade *et al.*, 2007). If optically thick clouds obstruct the sun, global irradiance can be reduced appreciably. On the other hand, clouds close to the apparent position of the sun, without occluding it, strongly scatter direct solar radiation, which may substantially enhance diffuse irradiance at the ground. In addition, atmospheric irradiance is determined mainly by radiation from the cloud-base regions, and the radiation reflects their temperature. Therefore, low clouds with higher temperatures emit more radiation than the cloudless sky (Feister and Shields, 2005). Hence, atmospheric conditions affect the overall intensity and spectral characteristics of solar illumination (Curtiss and Goetz, 1999). For example, aerosols increase and precipitable water decreases the reflectance in each spectral band (Tashiiri, 2005) and makes reliable measures difficult (Huete and Jackson, 1988). Therefore, atmospheric correction algorithms were developed (e.g. Kneizys *et al.*, 1988; Richter, 1996; Vermote *et al.*, 1997) and are still in the scope of recent studies (Tashiiri, 2005; Mahiny and Turner, 2007; El Hajj *et al.*, 2008) as a need for analysing airborne and satellite data.

For ground based measurements a standardised data record under stable cloud free and sunny conditions is required to reduce weather impacts (e.g., Schmidt and Skidmore, 2003; Mutanga *et al.*, 2004; Fitzgerald *et al.*, 2006; Jain, *et al.*, 2007). Particularly for ecological and agricultural research, where data collection is dependent on the growing season, difficulties will be encountered when routine ground based measurements are considered (Reusch, 2005). Therefore, to obtain data under changing conditions, the synchronistic measurement of the incoming global irradiance and of vegetative spectral response (Reusch, 2005; Leuning *et al.*, 2006; Larsolle and Hamid Muhammed, 2007) or additional light sources (Reusch, 2003; Lawrence *et al.*, 2007) provide perspectives for reliable data acquisition.

Nevertheless, only few reports are known presenting ground based in-field measures of how clouds affect hyperspectral data. Huete and Jackson (1988) simulated atmospheric conditions, Milton and Goetz (1997) analysed the short-term variability of the atmosphere by variations of white reference measurements, and Reusch (2005) recorded spectra of wheat under changing cloudiness. The degree of sky cover was estimated synoptically.

To obtain a better understanding of how clouds affect ground based hyperspectral measurements of forage crops, with their own specific vegetative and spectral characteristics, systematic investigations are still needed. These are aggravated by a high spatial and temporal variability of clouds, and hence, a permanent change of incoming solar radiation. Therefore, in this article, a binary forage sward of red clover and Italian ryegrass was analysed at different growth stages as a function of artificial darkening levels to systematically examine the effects of sky cover on the determination of biomass yield, crude ash (CP) and ash content (ash), as well as metabolisable energy (ME). In a second step an artificial halogen lamp was added over the measurement plots to examine the influence of additional illumination on the determination of the same crop constituents under changing weather conditions.

## 5.2 Material and methods

### 5.2.1 Experimental design and reference data

The field experiment was conducted during the year 2008 on the organic experimental farm Neu Eichenberg of the University of Kassel (51°21'N, 9°52'E, 240 m a.s.l.). Rainfall and temperature averaged 672 mm and 10.0°C, respectively. A binary mixture of red clover (*Trifolium pratense* L.) and Italian ryegrass (*Lolium multiflorum* L.) was investigated. The experimental tracts (3m x 80m) were established on 30th August 2007. In 2008 measurements were carried out at seven dates with a minimum of three replications from 28th April until 23th June over 0.25 m<sup>2</sup> plots. Due to technical problems, at the first measurement date only clear sky and total shaded spectra with six replications were recorded. In the following, all darkening levels were recorded, comprising three replications.

Sward height above soil was obtained by measuring red clover and Italian ryegrass separately using a meter rule. To define plant development the BBCH scale according to Meier (2001) was used. Growth stages are represented by two digits, i.e. germination (01-10), leaf development (11-20), formation of side shoots/tillering (21-30), stem elongation or rosette growth, (31-40), development of harvestable vegetative plant parts or vegetatively propagated organs/booting

(41-50), inflorescence emergence/heading (51-60), flowering (61-70) and development of fruit (71-80).

Total biomass was determined after spectral measurements, cutting a 0.25 m<sup>2</sup> plot at a height of 5 cm above soil surface. Samples were dried at 65°C for a minimum of 72 h. To obtain contents of the quality parameters, reflectance spectra of NIRS measurement were generated using a XDS-spectrometer (Foss NIRSystems, Hillerød, Denmark). The spectrum of a sample was an average of 25 subs cans and was recorded as the logarithm of the inverse of the reflectance ( $\log(1/R)$ ). Quality parameters were determined by already existing modified partial least squares (MPLS) calibrations (Loges, 1998) with the prediction accuracy in cross-validation of 89, 72, and 85 % in the nutritive values CP, ash and ME, respectively. The calculation was done with the WinISI software (version 1.63, Foss NIRSystems/Tecator Infracsoft International, LLC, Silver Spring, MD, USA), using the range between 1100 and 2498 nm.

### 5.2.2 Spectral data collection

Spectral measurements were conducted with a FieldSpec® 3 (Analytical Spectral Devices, CO, USA). This type of field spectrometer measures light energy reflected from swards in the range from 350 to 2500 nm with a spectral resolution of 3 nm (350-1000 nm) and 10 nm (1000-2500 nm). Measurements were then interpolated by the Analytical Spectral Devices (ASD) software RS3™ to produce readings at an interval of 1 nm. The sensor optic had a field of view of 25°, which was stabilised on a tripod in a height of 1.50 m above soil. Readings were taken on unclouded atmospheric conditions between 10:00 and 14:00 h Central European Time.

For the second experimental series a halogen bulb (1000 W; Fa Varo, Whitehall, UK) was established horizontally over the measurement plots at the same height as the sensor (Künne Meyer *et al.*, 2001), and the plots were measured again. Considering changing light conditions due to darkening levels and additional light, instrument optimisation and calibration was carried out prior to each measurement using a Spectralon panel. Each radiometric data point represented a mean of four measurements consisting of 40 replicated scans.

### 5.2.3 Determination of darkening levels for simulating different degrees of sky cover and signature of the artificial illumination source

To obtain five stages of cloudiness, defined as percental reduction of incident light, a 1.55\*1.55\*1.80 m<sup>3</sup> rack was adjusted over the measurement plots and covered with different layers out of cotton, totally enclosing the plots. While the material for the first darkening level was characterised by a wide meshed structure, the material for the remaining darkening levels was small meshed. Thereby, the reduction of incoming radiation was achieved by putting several layers upon the other. The darkening levels were determined in pre-tests by instrument calibration under cloud free, stable weather conditions and measuring the swards under the covered rack at noon time. Additionally, standard measurements were obtained by instrument calibration and target measurement under cloud free, sunny conditions without any shading. Therefore, 200 spectra for each darkening level and the standard measurement were recorded. Spectra of each darkening level were averaged and subsequently integrated over the same spectral range used for analysis, using the GRAMS/AI software, version 7.02 (Thermo Galactic, Woborn, MA, USA). Assuming that the reduction in reflectance measured under the rack equalled the reduction of global irradiance under defined degrees of sky cover, the percentage of incident light compared to the standard measurement was calculated by

$$\% \text{ Radiance} = A_{DL}/A_{SM} * 100, \quad (5.1)$$

with A for area under the integrated spectra at each darkening level (DL) and the standard measurement (SM).

The calculated percental reduction of incident light compared to standard measurements constituted 0, 33, 51, 67, and 74, respectively (Figure 5.1). In the following these darkening levels will be named as R100 (standard measurement) R67, R49, R33, R26, respectively, where R stands for radiance. Furthermore, sunlight was completely excluded by totally shaded measurement plots and spectra were recorded with artificial illumination only (R0). Transferring these meas-

ured reductions of reflectance to real sky conditions, the darkening levels relate to cloudy sky (R67), strongly cloudy sky (R49), nearly overcast sky (R33), overcast sky (R26) conditions (Berg, 1948; Hasenfratz, 2006), and night-time measurements (R0), respectively.

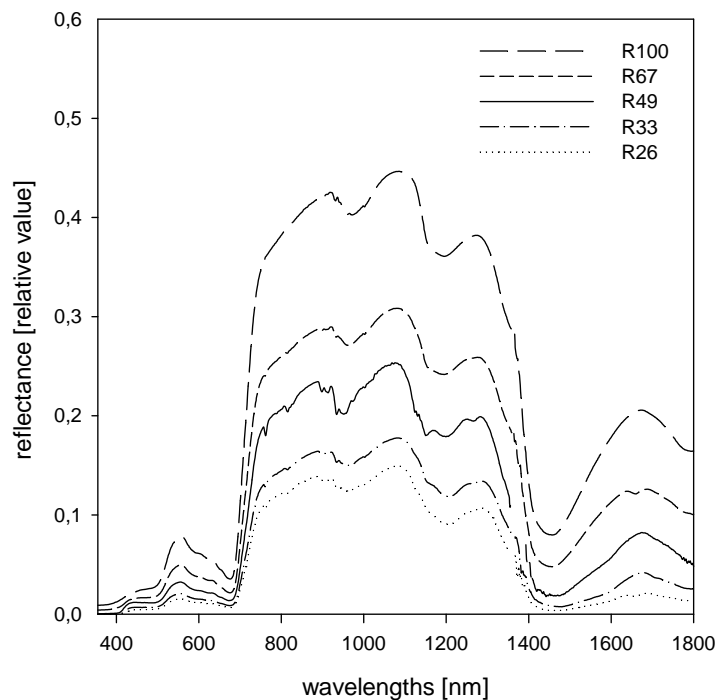


Figure 5.1: Reduction of reflectance under four different darkening levels (R67 – R26) compared to the standard measurement (R100) (spectra are exempt from stray light effects and water band noise at 1400 nm).

In a next step, the applicability of the chosen artificial illumination source was pretested by recording energy curves in the radiance mode with the FieldSpec® 3 in the laboratory. The halogen bulb was chosen to enable the illumination of the whole measurement plot with only one additional illumination source in order to minimise electrical setup in the field. Important for the applicability of an artificial illumination source is the provision of sufficient energy in the NIR region (Heege *et al.*, 2008). Therefore its energy curve was compared to those of a standard tungsten quartz halogen lamp (50 W, Analytical Spectral Devices, CO, USA), which is recommended by the manufacturer. The pre-test was carried out by positioning the sensor and the lamps horizontally one meter above a Spectralon panel (Labsphere, Inc., North Sutton, NH, USA). The chosen lamp emitted a smooth energy curve with its maximum at 1100 nm, slightly shifted to longer

wavelengths relative to the standard lamp. Regarding the entire spectrum, the chosen lamp provided sufficient energy compared to the standard lamp, and hence, was acceptable for field application.

#### 5.2.4 Analysis of spectral data

Prior to spectral analysis, spectra were smoothed using eleven convoluting integers and a polynomial of degree five (Savitzky and Golay, 1964, Erasmi and Dobers, 2004). In the first data set (without artificial light) four wavelengths regions were visually identified and omitted due to instrument noise and stray light effects (350 - 420 nm, 1950 - 2500 nm) or high atmospheric water absorption (1350 - 1475 nm, 1785 - 1950 nm). In the second data set (with artificial light), only two wavelengths regions were omitted (350 - 420 nm, 1785 - 2500 nm).

Subsequently, modified partial least squares (MPLS) regression was conducted, which is a method employed for data compression by reducing the large number of measured collinear spectral variables to a few non-correlated latent variables or factors (Cho *et al.*, 2007). As in multiple regressions, the main purpose of MPLS is to build a linear model:

$$y = b_1x_1 + b_2x_2 + \dots + b_nx_n + e \quad (5.2)$$

Y refers to the response variable (biomass in this study), x is the predictor variable (here the spectral wavelengths reduced to independent factors), b indicates the regression coefficients and e are the residuals (Geladi and Kowalski, 1986). The MPLS equations were developed using the WinISI software (version 1.63, Foss NIRSystems/Tecator Infracore International, LLC, Silver Spring, MD, USA).

For MPLS analysis parameters in the mathematical processing were identified by carrying out a trial-and-error procedure, in order to minimize the standard error of cross-validation (SECV). Therefore, no, 1st and 2nd derivative were combined with gaps and smooths of 0, 2, 4, 6, 8 and 10, comprising 44 calibrations for each darkening level.

Calibrations were carried out for single data sets (R100 with and without artificial light, including 24 samples) and over all darkening levels with 96 samples (R100 – R26 without artificial light) and 120 samples (R100 – R0 with artificial light), respectively, simulating changing sky cover. Every 2<sup>nd</sup> wavelength was used for the calculation of MPLS in order to reduce loss of information. Hence, 622 wavelengths were available for calibration for the data sets with and without artificial light, respectively.

Table 5.1: Averaged growth stages and sward heights (cm) of red clover and Italian ryegrass and descriptive statistics of DM yield (t/ha), CP (%), ash (%) and ME (MJ/(kg DM))

measurement	DOY	BBCH		sward height		DM yield	CP	ash	ME
		R.C.	I.R.	R.C.	I.R.				
1	119	17	17	7	10	0.5	21.9	9.7	12.2
2	136	22	23	16	20	1.0	17.8	8.9	12.1
3	141	35	32	32	44	2.7	16.0	9.3	11.6
4	154	39	49	21	76	3.7	9.7	7.6	10.4
5	162	52	53	59	109	4.0	8.6	6.1	10.1
6	169	39	58	30	101	4.1	6.6	5.2	10.4
7	175	33	65	35	97	5.6	7.4	4.6	10.2
min.		14	14	3	5	0.4	5.3	3.7	9.9
max.		62	67	72	112	6.5	23.1	11.0	12.3
mean		-	-	-	-	2.8	13.7	7.6	11.1

DOY: day of year; BBCH: phenological growth stages (Meier, 2001); R.C.: red clover; I.R.: Italian ryegrass; DM yield: mean dry matter yield (t/ha) per measurement date; CP: mean crude protein (% of DM) per measurement date; ash: mean crude ash (% of DM) per measurement date; ME: mean metabolisable energy (MJ/(kg DM)) per measurement date; min.: minimum; max.: maximum.

Cross validation was performed on the data sets. Therefore the data set was divided into six groups. One group was used for predicting while the rest was provided for developing the model. The procedure was performed until all samples were used for both model development and prediction. The number of factors giving the lowest final SECV determined the optimal number of terms to be used for the calibration and hence avoided an overfitting due to too many factors, which reduces the validation performance. Two outlier elimination passes were conducted, removing T outliers ( $T > 2.5$ ), characterised by a large difference between the reference and predicted values, and H outliers ( $H > 10$ ), i.e. samples whose spectra differed notably from the mean sample spectrum. Accuracy of the calibra-



tion models was assessed based on the standard error of cross validation (SECV), the coefficient of determination for cross validation ( $RSQ_{cal}$ ) and the RSC, defined by the ratio of standard deviation and SECV. Finally, each darkening level was used as a validation set to examine the prediction accuracy for a defined weather condition. Accuracy of the validation was assessed based on the standard error of prediction (SEP), the coefficient of determination for the linear regression ( $RSQ_{val}$ ) and the RPD, defined by the ratio of standard deviation and SEP. The stability factors RSC and RPD, respectively, characterise the robustness of a calibration equation and provide a comparison of the performance of all calibrations irrespective of the units of the investigated parameters (Park *et al.*, 1997). An RSC or RPD value greater than three is considered adequate for analytical purposes in most of the laboratory near infrared applications for agricultural products (Cozzolino *et al.*, 2006). However, at field scale variable measurement conditions reduce prediction accuracy, so that somewhat lower RSC or RPD values may indicate good results. According to Therhoeven-Urselmans *et al.* (2006) good prediction results are given in laboratory for organic matter in soil and litter, if RSC or RPD is higher than 2.

### **5.3 Results and discussion**

#### **5.3.1 Sward characteristics, DM yield and quality parameters**

As swards were investigated at various growth stages ranging from leaf development (BBCH 17) to finishing of flowering (BBCH 67), DM yield varied from 0.4 to 6.5 t/ha (Table 5.1). Due to the late sowing date (August 30, 2007) and a drought period after sowing, sward establishment was constricted. As a result swards held high amounts of visible soil at the beginning of the measurement period. Furthermore, red clover was partly suppressed by quickly elongated grass plants in spring (Table 5.1). Therefore, sward height varied between 20 cm for red clover and 100 cm for Italian ryegrass at the later measurement dates. Red clover scarcely reached flowering stage (BBCH 62) and canopy structure was very heterogeneous. Crude protein (CP) content varied from 5.3 to 23.1 % of DM and decreased during the measuring period continuously, as did ash and ME. These

constituents varied from 3.7 to 11.0 % DM, and from 9.9 to 12.3 MJ/(kg DM) for ash and ME, respectively (Table 5.1).

### 5.3.2 Spectral signatures in response to darkening levels and illumination

Due to the experimental design with the instrument calibration and target measurement under the same illumination conditions, spectral responses at the same relative level were expected for all darkening levels of a measurement plot. This assumption was approved by the second and partly by the third and fourth measurements without additional light, where the sward was still low and the growth stages of red clover and Italian ryegrass equalled (Figure 5.2). With increasing diversification of the sward architecture the spectral response in the NIR region expanded, whereas the spectra in the visible band did not show significant diversification. The average reflectance of mature swards was increased by 17 % for R33 and R49 and by 25 % for R26 compared to R100 and R67 in the near infrared and shortwave infrared bands (700 – 1350 nm), where spectral diversification was strongest (Figure 5.2b), indicating that the spectral response was increased with the reduction of incident solar radiation. These findings are related with the complex structure of canopies, including plant height, and thus number of leaf layers (Bauer, 1985; Zwiggelaar *et al.*, 1998), as well as canopy density (Huete and Jackson, 1988; Hansen and Schjoerring 2003). In this study, the fabric layers of R49, R33 and R26, used to simulate different conditions of sky cover, trapped incoming solar radiation and scattered it back to the canopy where the radiation was reflected again. This multiscatter effect was enhanced by the canopy density and number of leaf layers for advanced growth stages and was pronounced in the NIR band, where spectral response was highly dependent on the intercellular leaf structure (Jensen, 2000). However, relative reflectance equalled for R49 and R33 (one and two layers small meshed fabrics, respectively) and was enhanced for R26 (five layers small meshed fabrics) compared to R100 and R67, which indicated a dependency on the number of fabric layers. Nevertheless, although the results showed an interaction with the artificial darkening levels, the multiscatter effect was only detectable, when sward architecture became heterogeneous and the sward components developed their own characteristic light-interaction pattern

(Nassiri and Elgersma 1998; Lantinga *et al.*, 1999). These findings correlate with natural atmospheric conditions, where ground measured irradiance is enhanced due to clouds close to the apparent position of the sun. Particularly, the atmospheric irradiance in the infrared region is influenced by the temperature of its atmospheric source region, and hence, determined mainly by radiation from the cloud-base regions, where the radiation reflects their temperature (Feister and Shields, 2005). Therefore, low clouds with higher temperatures emit more radiation than the cloudless sky, that can exceed more than 500 W/m<sup>2</sup> compared to clear sky irradiation (Schade *et al.*, 2007) and can last up to an hour (Segal and Davis, 1992). Furthermore, Schade *et al.* (2007) found maximal enhancements of radiation at nearly overcast situations with altocumulus clouds partly obscuring the solar disk. Hence, these findings explain the diversification of spectra, as well as the increasing spectral response with increasing sky cover in the NIR bands.

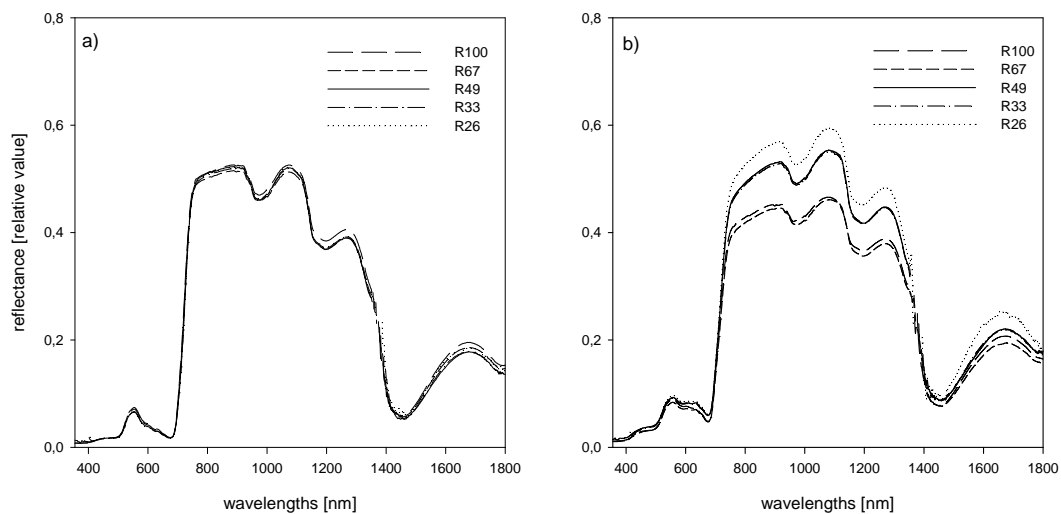


Figure 5.2: Measured spectra of defined darkening levels (R67-R26) compared to clear sky conditions (R100). a) DOY 141, b) DOY 175 (white reference and measurements were conducted under the rack).

In a second step a halogen lamp was established over the measurement plots to test the influence of artificial light on spectra recorded under turbid weather conditions i) in combination with natural illumination and ii) by excluding solar radiation (Figure 5.3). The relative reflectance of artificially illuminated swards is clearly reduced compared to those under solar illumination. This was ascribed to the experimental set up, since the spectralon panel, used for instrument calibration, was fixed approximately 10 cm under the sensor and hence, was very close

to the lamp, which led to indifferent illumination conditions for instrument calibration and target measurement. The lambertian surface for collecting the white reference was lit up very brightly compared to the canopy examined beneath. As the data recorded was the ratio of the spectral responses of the target and the white reference, the white reference data was overestimated and the relative reflectance was low.

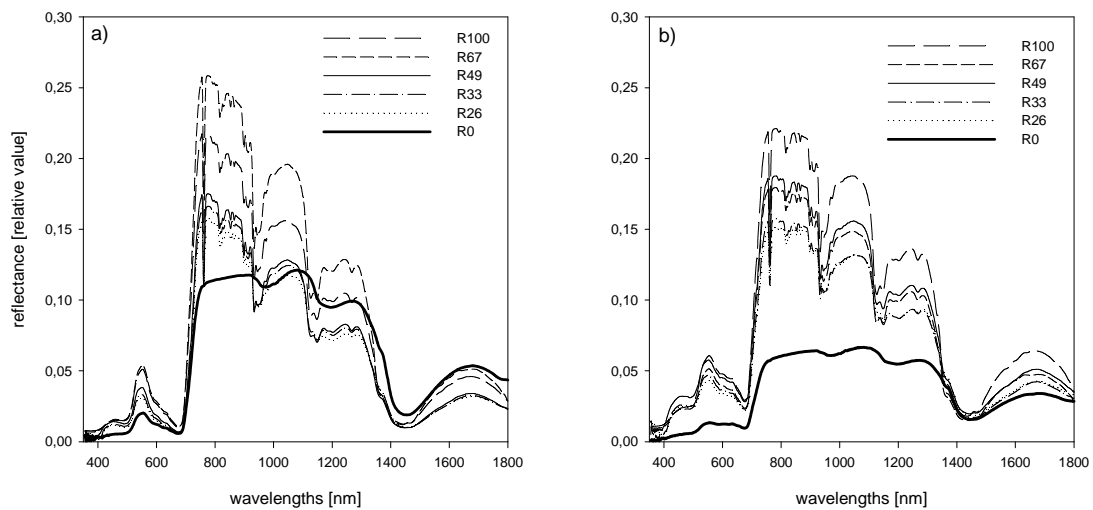


Figure 5.3: Measured spectra of defined darkening levels (R67-R0) compared to clear sky conditions (R100) using artificial illumination. a) DOY 141, b) DOY 175 (white reference and measurements were conducted under the rack).

Unlike to natural illumination conditions, where spectral response increased with the degree of induced cloudiness, the spectral response of artificially illuminated swards decreased with the degree of induced sky cover. With the Spectralon panel very close to the halogen lamp, the fraction of artificial light, that illuminated the Spectralon panel to record the white reference, was clearly increased compared to the solar radiation component. In contrast, recording the target, the artificial illumination energy was relatively low, due to the diffusion of light. Hence, the spectral response of the target was much more dependent on the fraction of solar radiation, which was reduced stepwise by the darkening levels. This led to a decrease of the spectral response with increasing shadowing independent on sward maturity and to a masking of the multiscatter effect, found with solar illumination.

The pronounced peaks in spectra with combined illumination compared to spectra without additional light and pure artificial illumination spectra (R0) is another

noteworthy difference. This optical phenomenon occurred in spectral bands known as minor water absorption bands around 720, 820, 940 and 1120 nm, respectively (Hatchell, 1999; Oppelt, 2002). The present study cannot fully explain the reasons for these spectral extinctions, but it is assumed that the effects are related with optical path differences of the solar and artificial light sources. This assumption is supported by the spectra resulting from one illumination source only, since the interferences do not occur under natural illumination or when the sunlight is excluded (R0), where spectra showed a smooth characteristic (Figure 5.3). As these phenomena occurred for all measurements with artificial light equally, the spectral data can be used for developing calibrations in this study.

### **5.3.3 Relationships between prediction accuracy of dry matter yield, nutritive values and simulated sky cover with solar and artificial illumination**

#### ***Dry matter yield***

To determine the influence of illumination conditions on prediction accuracies for DM yield the best cross-validation results for data sets with and without additional light were compared (Table 5.2). No scatter correction was best for R100 and for overall calibrations without artificial illumination. In contrast, to obtain adequate results for artificially illuminated measurements, SNV-Detrend and SNV scatter correction were required. This is related to the strong amplification of water absorption features in the artificially illuminated spectra.

Cross-validation and RSC values proofed robust calibrations, although data sets of R100 measurements were small with only 24 samples (Table 5.2, Figure 5.4 a, b). These results are in line with former studies without additional light sources, where biomass was predicted good to very good (e. g. Thankabail *et al.*, 2000; Serrano *et al.*, 2000; Biewer *et al.*, 2009b). Regarding measurements with additional lightning, Lawrence *et al.* (2007) and Reusch (2005) reported high prediction accuracies for fecal contaminant detection and N-uptake, respectively, using LED and halogen-tungsten bulbs. In contrast, Künnemeyer *et al.* (2001) reported poorer calibrations for green biomass with additional light using LEDs. The use of LED bulbs which are characterised by discontinuous spectra, presumes the

knowledge of the spectral bands correlated with the defined constituent, since otherwise prediction accuracy may be low (Lawrence *et al.*, 2007; Heege *et al.*, 2008).

Table 5.2: Statistics of the cross-validation for DM yield (t/ha) for clear sky conditions and the overall calibrations with and without artificial light. The best scatter corrections and math treatments for the cross-validation, the standard errors of cross-validation (SECV), the coefficient of determination ( $RSQ_{cal}$ ) of the cross validation and the stability factor RSC are given.

Darkening level	n	scatter correction	mathematical treatment*	SECV	$RSQ_{cal}$	RSC <sup>o</sup>
without artificial light						
R100	23	none	1 6 6	0.68	0.86	2.7
R100 – R26	96	none	1 10 10	0.62	0.87	2.7
with artificial light						
R100	23	SNV-Detr.	2 6 6	1.01	0.73	1.9
R100 – R0	114	SNV	1 8 8	0.64	0.87	2.8

\*The first number of the math treatment is the order of the derivative function, the second number is the segment length in data points over which the derivative was taken, the third is the segment length over which the function is smoothed. <sup>o</sup>RSC: ratio of standard deviation and SECV

In a next step, the influence of sky cover on the prediction accuracy was examined by validating R67, R49, R33 and R26 data sets using the R100 calibration equations (Table 5.3). For solar illumination the prediction accuracy decreased, the more the simulated cloudiness increased, represented by increasing SEP and decreasing  $RSQ_{val}$  and RPD, respectively. In contrast, the results under artificial lighting were poor for R67, R49 and R33 with low  $RSQ_{val}$  and RPD values. Results were improved for R26, when solar radiation was excluded to over 80 %. This significant increase in prediction accuracy was probably based on the reduced amount of incoming solar radiation and thus a reduction of interferences of solar and artificial light in this study.

The overall calibrations were conducted to study the prediction accuracy of constituents under a wide range of weather conditions (Table 5.2, Figure 5.4 c, d). This approach was based on NIR-spectroscopy practise, where multiple measurements of one sample were included in calibration developments to increase spectral variance (Moschner, 2007). Aside a good correlation, samples of different darkening levels were equally distributed along the bisecting line. Hence, prediction of DM yield seems to be possible under changing weather conditions, pro-

vided that instrument calibration and target measurement are conducted under the same illumination conditions. However, ambient illumination conditions hardly

Table 5.3: Statistics of the validation of DM yield (t/ha) for each darkening level, based on clear sky calibration models with and without artificial light. The standard error of prediction (SEP), the coefficient of determination ( $RSQ_{val}$ ) of the linear regression and the stability factor RPD are given.

Darkening level	SEP	$RSQ_{val}$	RPD <sup>o</sup>
without artificial light			
R67	0.89	0.76	1.8
R49	1.36	0.60	1.2
R33	1.51	0.54	1.1
R26	3.65	0.17	0.4
with artificial light			
R67	1.20	0.51	1.4
R49	1.19	0.53	1.4
R33	1.24	0.47	1.3
R26	0.84	0.77	2.0

<sup>o</sup>RPD: ratio of standard deviation and SEP

reach this simulated, stable cloudiness due to short term changes of global radiance in presence of clouds (Huete and Jackson, 1988; Milton and Goetz, 1997; Feister and Shields, 2005). To correct these impacts of short-term variation in sky cover the simultaneous measurement of incoming solar irradiation maybe have potential, as already implemented e.g. by Reusch (2005) or Larsolle and Hamid Muhammed (2007).

### ***Quality parameters CP, ash and ME***

Cross-validation procedures were conducted to obtain best calibration results for CP, ash and ME, comparing overall calibrations with (R100-R0) and without (R100-R26) artificial light (Table 5.4). All samples deleted for calibration were T-outliers. Outlier elimination was highest for ash under artificial lightning with eight deleted samples. The RSC values indicated robust calibrations, ranging between 2.7 (CP with artificial light) and 4.0 (ash with and without artificial light). In both data sets CP could be predicted poorest with  $RSQ_{cal}$  of 0.87 for R100-R0

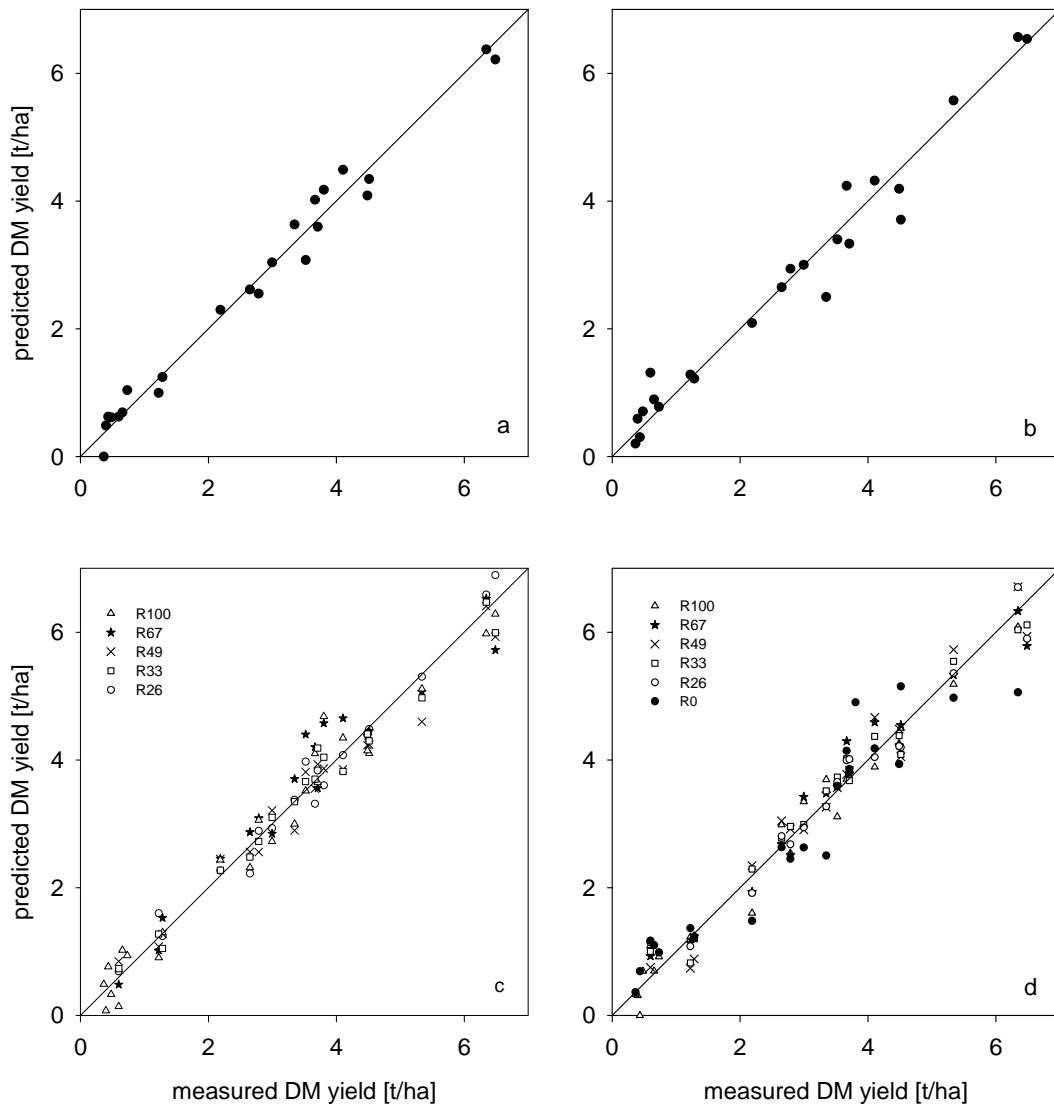


Figure 5.4: Measured and predicted values of DM yield [t/ha] under clear sky conditions (R100) a) without artificial light, b) with artificial light and under changing sky covers c) without artificial light and d) with artificial light. Lines indicate  $y=x$ .

with artificial illumination and of 0.91 for R100-R26 without additional light. Calibrations for ME and ash were slightly better with maximum  $RSQ_{cal}$  values of 0.94 (ash with and without artificial light). Prediction accuracy was improved under natural illumination conditions compared to combined lightning for CP and ME (Figure 5.5). This is ascribed to the interferences of solar and artificial radiation pronouncing irregularities in the spectra. Differences in prediction accuracy could not be found for ash, where results were equal for both, solar and combined illumination data sets. The detection of the mineral portion of plants is strongly



related to chelate complexes connected to organic compounds and hence, the NIRS

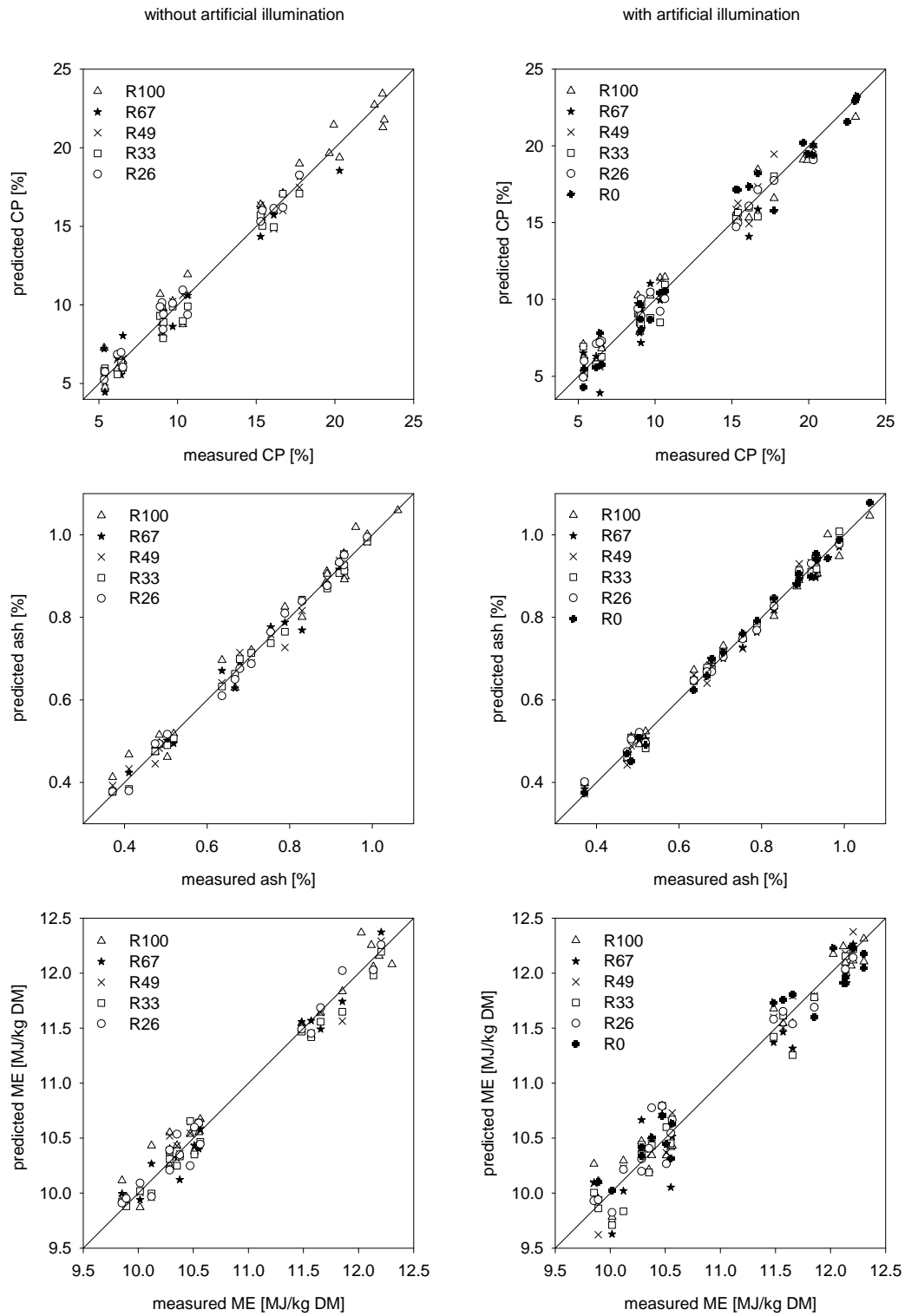


Figure 5.5: Measured and predicted values of CP [%], ash [%] and ME [MJ/kg DM] under changing sky covers with (R100-R0) and without (R100-R26) artificial light. Lines indicate  $y=x$ .

does not directly measure the element, but the organic compound the element is related to (Park *et al.*, 1998; González-Martín *et al.*, 2007). This offers a multitude of spectral bands correlated to ash and the dependency of calibration development on spectral interferences near the minor water absorption features is attenuated.

Biewer *et al.* (2009c) also examined binary mixtures of grass and clover under clear sky conditions using the field spectroscopy. These authors reported similar results for ash and crude protein but poorer results for ME, which they ascribed to a small range of variance of the reference data.

Table 5.4: Statistics of the cross-validation for CP (%), ash (%) and ME (MJ/(kg DM)) for overall calibrations with and without artificial light. The best scatter corrections and math treatments for the cross-validation, the standard errors of cross-validation (SECV), the coefficient of determination ( $RSQ_{cal}$ ) of the cross validation and the stability factor RSC are given.

constituent	n	scatter correction	mathematical treatment*	SECV	$RSQ_{cal}$	RSC <sup>o</sup>
without artificial light (R100 – R26)						
CP	93	none	1 8 8	1.51	0.91	3.3
ash	93	none	2 8 8	0.49	0.94	4.0
ME	94	none	1 8 8	0.23	0.92	3.5
with artificial light (R100 –R0)						
CP	115	SNV	2 10 10	1.95	0.86	2.7
ash	112	MSC	1 2 2	0.48	0.94	4.0
ME	118	none	1 10 10	0.28	0.91	3.4

\*The first number of the math treatment is the order of the derivative function, the second number is the segment length in data points over which the derivative was taken, the third is the segment length over which the function is smoothed. <sup>o</sup>RSC: the ratio of standard deviation and SECV

Prediction accuracy of field spectroscopic measurements regarding RSQ and RPD values for the prediction of CP, ash and ME was similar to spectroscopic measurements under standardised conditions in the laboratory (e.g. Park *et al.*, 1998; Volkers *et al.*, 2003; Cozzolino *et al.*, 2006), and hence, sensor based detections of canopy parameters, obtained in the field, could be a fast and reasonable alternative to labour and cost intensive laboratory analysis.

## 5.4 Conclusions

The experiments were conducted to achieve an improved understanding of how solar and artificial illumination influence canopy reflectance and prediction accuracies in field spectroscopy. Although evidence of interactions between measure-

ment set up and spectral response was found, the following main conclusions can be drawn:

- i) An increase of sky cover results in an enhanced spectral response of the canopy, particularly in the NIR band, when sward architecture becomes heterogeneous.
- ii) Prediction accuracy of DM-yield decreases with increasing degree of sky cover using clear sky calibration without artificial lightning. In contrast, the accuracy increased with increasing degree of sky cover using clear sky calibration with artificial lightning, due to exclusion of solar radiance.
- iii) Overall calibrations, comprising data recorded under simulated degrees of sky cover, showed very good results for DM, CP, ash and ME.
- iv) Nevertheless, calibration development only is reliable, if instrument calibration and target record is performed under stable illumination conditions or with the simultaneous measurement of incoming solar radiation.

The results promise the adaptability of hyperspectral measurements for the prediction of dry matter yield and nutritive values in grass-clover mixtures regarding heterogeneous weather conditions. However, to reduce spectral interactions due to the experimental set up, these findings have to be verified in a further experiment using ambient illumination conditions.

## **6 Off-nadir hyperspectral measurements in maize. Comparison of different angle-height combinations for on-the-go-solutions to predict DM yield, protein and ME contents in total biomass.**

**Abstract** Sensor based analysis methods to assess dry matter yield and quality parameters of crops are time and labour saving and can facilitate a site-specific management. Nevertheless, standard nadir measurements in maize (*Zea mays* cv. Ambrosius), based on top of canopy reflectance, are difficult due to plant heights of more than three meters. This study was conducted to explore the potential of off-nadir field spectral measurements for a non destructive prediction of dry matter yield (DM), metabolisable energy (ME), and crude protein (CP) in total biomass, inside a maize canopy. Plants were measured in five different height segments (0 – 50 cm, 50 – 100 cm, 100 – 150 cm, 150 – 200 cm, and 200 – 250 cm, respectively) under three zenith view angles (60°, 75°, and 90°, respectively). Modified partial least squares (MPLS) regression was used for analysis of the hyperspectral data set (355 – 2300 nm and 620 – 1000 nm). Combination of angle and height for all parameters in total biomass were determined as well as an optimum one-sensor-strategy for all three constituents. Coefficients of determination ( $RSQ_{cv}$ ) obtained by off-nadir measurements were compared to nadir measurements, resulting in improved prediction accuracies for DM yield and ME using off-nadir application. In contrast, prediction accuracy for CP could hardly be reached with off-nadir adjustments compared to nadir measurements.

**Keywords:** maize, biomass yield, forage quality, field spectroscopy.

## 6.1 Introduction

The application of remote sensing techniques has increased consistently in the last few years in crop management systems. Essential components of precision agriculture are methods of obtaining and mapping of factors influencing productivity as well as spatial and temporal variabilities (Goel *et al.*, 2003). Data derived from satellite based sensors such as Landsat TM/ETM+ and AVHRR are characterised by either few spectral bands or spatial resolutions often too low for site specific applications in agriculture (Goel *et al.*, Cho *et al.*, 2007). Furthermore, many approaches focus on developing empirical relationships between ground measured vegetation parameters and calculated vegetation indices (VIs), only using a small part of the potential of hyperspectral remote sensing data (Erasmi and Kappas, 2003). There are major limitations with VIs despite their wide application in agronomical remote sensing, since these techniques often ignore the causal context between spectral reflectance, crop variables and external effects such as varying soil colour, canopy structure, leaf optical properties, sensor view geometry and atmospheric conditions (Qi *et al.*, 1995; Todd *et al.*, 1998; Erasmi and Kappas, 2003). In contrast, most hyperspectral sensors record radiance information in less than 10 nm bandwidths from the visible (400-700 nm) to the short wave infrared (SWIR; 700-2500 nm) (e.g., Lee *et al.*, 2004; Starks *et al.*, 2008; Biewer *et al.*, 2009c) and hence, are a powerful and versatile tool for continuous sampling (Hansen and Schjoerring, 2003).

While data from airborne hyperspectral measurements such as AVIRIS are currently available only for scientific purposes, on-the-go applications are required in order to determine crop or soil status in real time and thus to minimize time and effort for agronomists (Heege *et al.*, 2008; Maleki *et al.*, 2008). For cereal crops, soil and intertillages these mobile applications are already available with sensors mounted on top of a tractor recording nadir and off-nadir top of canopy reflectance, respectively (Hansen and Schjoerring, 2003; Heege *et al.*, 2008; Maleki *et al.*, 2008). Off-nadir measurements provide further information on canopy structures and hence can yield in improved prediction accuracies for distinct target parameters (e.g. Sandmeier *et al.*, 1998; Los *et al.*, 2005).

For maize crops with plant heights of at least three meters technical limitations are reached considering the record of top-of-canopy reflectance as required by most field spectrometric applications. Furthermore, it is doubtful that top-of-canopy reflectance is able to represent adequately the nutrition status of high growing crops since reflectance only consists of top layer optical properties. However, maize is one of the most important forage crops worldwide and the increasing demand for renewable energy further expands the area used for maize production.

This study presents data of a three years lasting experiment recording off-nadir measurements inside a maize canopy using different angle/height combinations. The specific objectives of the study are

- (i) to evaluate the impact of angle and height on prediction accuracy,
- (ii) to determine prediction accuracies for dry matter yield (DM yield), crude protein (CP) and metabolisable energy (ME) using off-nadir data record inside a canopy, when reflectance of 50 cm segments of the plants are collected only in the entire (355 – 2300 nm) and reduced (620 – 1000 nm) wavelength range, and
- (iii) to find optimum angle-height-combinations to achieve highest prediction accuracies for a potential on-the-go application and compare those to nadir measurements recording top-of-canopy reflectance.

## **6.2 Material and methods**

### **6.2.1 Experimental design and reference data**

Organically managed field plots (12\*80 m<sup>2</sup>) of maize (*Zea mays* cv Ambrosius) were established on the experimental farm Neu Eichenberg of the University of Kassel (51°21'N, 9°52'E, 240 m a. s. l.) in 2006, 2007, and 2008. Maize was sown end of April/beginning of May with 75 cm row spacing at the rate of 100 000 seeds/ha. In 2006 row orientation was north-south, while in 2007 and 2008 row orientation was east-west.

Between the field plots a 5 m wide machine track was kept free in order to pass with the tractor for nadir measurements. Nadir measurements 0.5 m above the canopy were realised by establishing the sensor on a square tube telescope arm, installed on a front loader. In order to avoid fringe effects, spectral data of the fifth row of the field plots were recorded. Off-nadir measurements were carried out in-between the rows in five different height segments (0-50 cm; 50-100 cm; 100-150 cm; 150-200 cm; 200-250 cm) and three angles ( $60^\circ$ ,  $75^\circ$  and  $90^\circ$  zenith view angle). The sensor distance to the examined plant row varied between 0.65 and 0.90 m, depending on the geometric view angle of the sensor in order to record the same height segment of the plant (Figure 6.1). In 2006 and 2007, measurements were conducted at three dates from early milk-ripe stage to full ripe stage. In 2008 seven measurements were conducted including stem elongation to ripening. To define plant development the BBCH scale according to Meier (2001) was used. Growth stages are represented by two digits, i.e. germination (00-09), leaf development (10-19), stem elongation (30-39), inflorescence emergence/heading (51-59), flowering, anthesis (61-69), development of fruit (71-79), ripening (81-89) and senescence (91-99).

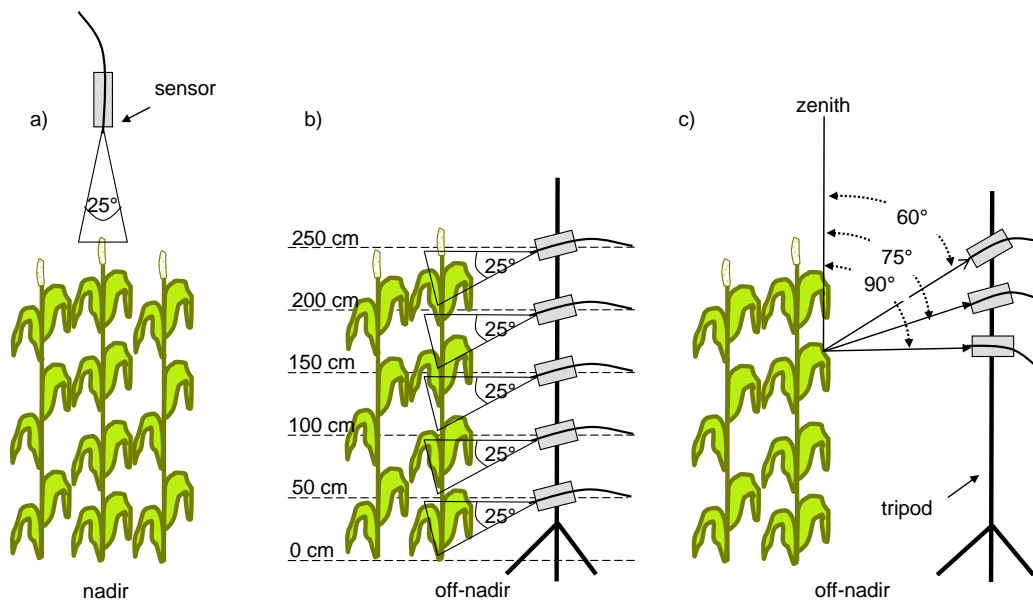


Figure 6.1: Schematic measuring setup for nadir (a) and off-nadir (b+c) measurements, including sensor field of view (a+b); segment heights (b) and zenith view angle (c).

Plant height above soil was obtained using a meter rule. Biomass of each height segment was determined after spectral measurements, cutting one meter of corn plants of the measured row separately in 50 cm segments according to the measurement heights. Samples were dried at 65°C for a minimum of 72 h. Total biomass was calculated by accumulation of biomasses from all segments. To obtain quality data, reflectance spectra of NIRS measurement were generated using a XDS-spectrometer (Foss NIRSystems, Hillerød, Denmark). The spectrum of a sample was an average of 25 subscans and was recorded as the logarithm of the inverse of the reflectance ( $\log(1/R)$ ). Quality parameters were determined by modified partial least squares (MPLS) calibrations developed from maize material published by Volkers *et al.* (2003) with a  $R^2$  of 0.97 for CP and ME, respectively. Predictions were conducted with the WinISI software (version 1.63, Foss NIRSystems/Tecator Infrasoft International, LLC, Silver Spring, MD, USA), using the range between 1100 and 2498 nm.

### 6.2.2 Spectral data collection

Spectral measurements were conducted with a FieldSpec® 3 (Analytical Spectral Devices, CO, USA). This type of field spectrometer measures light energy reflected from the canopy in the range from 350 to 2500 nm with a spectral resolution of 3 nm (350 – 1000 nm) and 10 nm (1000 – 2500 nm). Measurements were then interpolated by the Analytical Spectral Devices (ASD) software RS<sup>3</sup>™ to produce readings at an interval of 1 nm. The sensor optic had a field of view of 25°. Readings were taken when possible on unclouded atmospheric conditions between 10:00 and 14:00 h Central European Time. Instrument optimisation and calibration was carried out prior to the nadir measurements and prior to each angle adjustment holding the sensor in nadir direction over a horizontally orientated Spectralon panel. Each radiometric data point represented a mean of four measurements consisting of 40 replicated scans. Field measurements were conducted with three fully randomized replicates. Due to technical problems and unstable weather conditions, in 2006 and 2007 measurements were conducted partly with only one replication and occasionally spectra were obscured.



### 6.2.3 Spectra pre-processing

Spectra were smoothed using eleven convoluting integers and a polynomial of degree five (Savitzky and Golay, 1964, Erasmi and Dobers, 2004). Three wavelength regions were visually identified and omitted due to instrument noise (2301 – 2500 nm) or high atmospheric water absorption (1351 – 1449 nm, 1801 – 2029 nm).

### 6.2.4 Calculation of Simple Ratio vegetation index and analysis of variance

To examine differences of reflectance depending on angle/height adjustments, Simple Ratio (SR) vegetation index was calculated from the spectral dataset using the following equation (Biewer *et al.*, 2009a):

$$SR = \frac{R_{940}}{R_{640}}, \quad (6.1)$$

with R representing the reflectance value at wavelength 940 and 640, respectively.

Subsequently, SR was subjected to a multi-factorial analysis of variance using the GLM procedure of SAS 9.2 (SAS Institute, 2002 – 2008).

### 6.2.5 Cross-Validation

Modified partial least squares (Martens *et al.*, 1989) (MPLS) method was used to develop calibration equations using the WinISI software (version 1.63, Foss NIR-Systems/Tecator Infracore International, LLC, Silver Spring, MD, USA). This method was employed for data compression by reducing the large number of measured collinear spectral variables to a few non-correlated latent variables or factors (Cho *et al.*, 2007). For MPLS analysis parameters in the mathematical processing were identified by carrying out a trial-and-error procedure, in order to minimise the standard error of cross-validation (SECV). Therefore, no, 1st and 2nd derivative were combined with gaps and smooths of 0, 2, 4, 6, 8 and 10, as well as none, standard normal variate and detrending (SNV-D), and multiplicative scatter correction (MSC) procedures, comprising 45 calibrations for each angle-height combination. Every second wavelength was used for calculation of MPLS in order to reduce loss of information. Hence, 810 wavelengths were available in

the wavelength range from 355 to 2300 nm for calibration. In a second step the hyperspectral data were reduced to a range of 620 to 1000 nm due to the importance of red and short wave near infrared wavebands in detecting forage quality variables (Biewer *et al.*, 2009c). This range is adapted to the Yara N-sensor® (FS; Yara International ASA, Oslo, Norway) which is already used for site-specific fertilizer applications in practise.

Full cross validation was performed on the data set. Therefore samples were divided into six groups. One group was used for predicting while the rest was available for developing the model. The procedure was performed until all samples were used for both model development and prediction. The number of factors giving the lowest final SECV determined the optimal number of terms to be used for the calibration and hence avoided an overfitting due to too many factors (González-Martín *et al.*, 2007). Two outlier elimination passes were conducted, removing T outliers ( $T > 2.5$ ), characterized by a large difference between reference and predicted values, and H outliers ( $H > 10$ ), i.e. samples whose spectra differed notably from the mean sample spectrum.

Accuracy of calibration models was assessed based on standard error of cross validation (SECV), coefficient of determination for cross validation ( $RSQ_{cv}$ ) and RSC, defined by the ratio of standard deviation and SECV. The stability factor RSC characterises the robustness of a calibration equation and provides a comparison of the performance of all calibrations irrespective of the units of the investigated parameters (Park *et al.*, 1997). An RSC value greater than three is considered adequate for analytical purposes in most of the laboratory near infrared applications for agricultural products (Cozzolino *et al.*, 2006). However, at field scale variable measurement conditions reduce prediction accuracy, so that somewhat lower RSC values may indicate good results (Biewer *et al.*, 2009b). According to Therhoeven-Urselmans *et al.* (2006) good prediction results are given in laboratory for organic matter in soil and litter, if RSC is higher than 2.

## 6.3 Results and discussion

### 6.3.1 Canopy characteristics, DM yield and quality parameters

As maize canopy was investigated at various growth stages ranging from stem elongation (BBCH 34) to ripening (BBCH 89), DM yield varied from 3.5 to 21.8 t/ha. Crude protein (CP) content and metabolisable energy (ME) varied from 4.8 to 14.5 % of DM and 8.4 to 11.4 MJ/kg DM, respectively (Table 6.1). In 2006 and 2007 measuring period began at stage of milk ripening/development of fruits, while in 2008 measurement period began with stem elongation. The latter year was used to trace the variation of DM yield, CP and ME over the entire plant height and maturity progress (Figure 6.2). DM yield increased continuously with proceeding crop maturity, mainly induced by cob development and stem and leaf growth, respectively, in the lower parts of the plants.

The increase of biomass is associated with an enhancement in the proportion of plant structural and storage tissues during maturity process and hence, a decrease of leaf nitrogen concentration (Greenwood *et al.*, 1990; Plénet and Lemaire, 1999) which is directly correlated with CP. This time effect is combined with a vertical gradient from top to bottom within the canopy due to a vertical attenuation of light intensity. Hence, young leaves in the upper canopy layers accumulate more nitrogen to optimize photosynthesis due to the substantially smaller leaf area index (Plénet and Lemaire, 1999; Gastal and Lemaire, 2002; Mistele and Schmidhalter, 2008). Therefore, crude protein decreases from top to bottom of plants and from young to mature developmental stages (Figure 6.2).

On the one hand concentration of ME depends on plant ripening, where digestibility is negatively correlated with the increase of fibre in the plant material during the maturity process (Longe, 1989). At the same time digestibility increases with cob growth. This contrary development leads to an almost equal level of ME over the entire measurement period (Figure 6.2) and a shift of ME from the upper plant layers to the centre where maize cobs are located. These findings correspond with results presented by Pordesimo *et al.* (2005), who examined the content of gross energy (GE) over the vegetation cycle of maize.

Table 6.1: Averaged growth stages and canopy heights (cm) of maize (*Zea mays* cv Ambrosius) and descriptive statistics of dry matter yield (DM) [t/ha], crude protein (CP) [% DM], and metabolisable energy (ME) [MJ/kg DM].

measurement	DOY	BBCH	canopy height	n	DM yield			CP			ME		
					mean	min	max	mean	min	max	mean	min	max
2006													
1	219	71	230	5	7.4	0.2	3.3	9.5	3.5	15.9	9.8	7.0	11.0
2	250	83	235	5	11.9	0.4	8.6	5.6	5.4	10.9	11.0	6.6	13.6
3	255	87	235	14	11.5	0.1	10.0	6.3	0.9	13.3	11.4	5.9	13.4
2007													
4	218	73	250	15	14.3	1.5	5.4	6.9	2.2	15.6	8.4	5.6	10.5
5	237	82	250	15	21.8	1.3	13.2	6.9	3.2	12.4	8.5	5.4	10.1
6	262	89	280	15	21.8	1.0	12.9	5.5	2.4	13.6	9.6	5.1	12.0
2008													
7	183	34	140	15	3.5	1.4	2.1	14.5	12.7	17.4	10.3	10.0	10.5
8	197	55	245	15	9.5	0.4	2.8	9.2	4.8	18.1	9.5	7.7	10.7
9	205	63	290	15	13.0	1.3	3.8	7.5	3.8	12.8	8.7	5.5	10.3
10	210	71	305	15	16.9	1.9	5.6	7.0	3.7	12.9	9.0	6.2	11.0
11	220	75	295	15	16.1	0.9	8.2	5.5	1.0	13.2	9.3	7.4	10.3
12	234	81	280	15	20.1	1.2	10.4	5.7	1.0	11.3	9.8	6.5	12.4
13	244	85	290	15	21.5	1.3	11.8	4.8	1.4	9.1	9.0	6.2	12.0

DOY: day of year; BBCH: phenological growth stages (Meier, 2001); canopy height in cm; n: number of samples; mean: weighted mean for dry matter harvested per measurement date; min.: segmental minimum of measurement date; max.: segmental maximum of measurement date.

### 6.3.2 Dependency of reflectance on angle and height

Due to interactions of lighting conditions, plant architecture and constituent content spectral response varies with the level of height and angle (Figure 6.3). In order to test the effects of angle and height, as well as their interaction, on reflectance pattern, a multi-factorial analysis of variance was conducted using Simple Ratio (SR, eq. 6.1) vegetation index as dependant variable. This VI is known as a

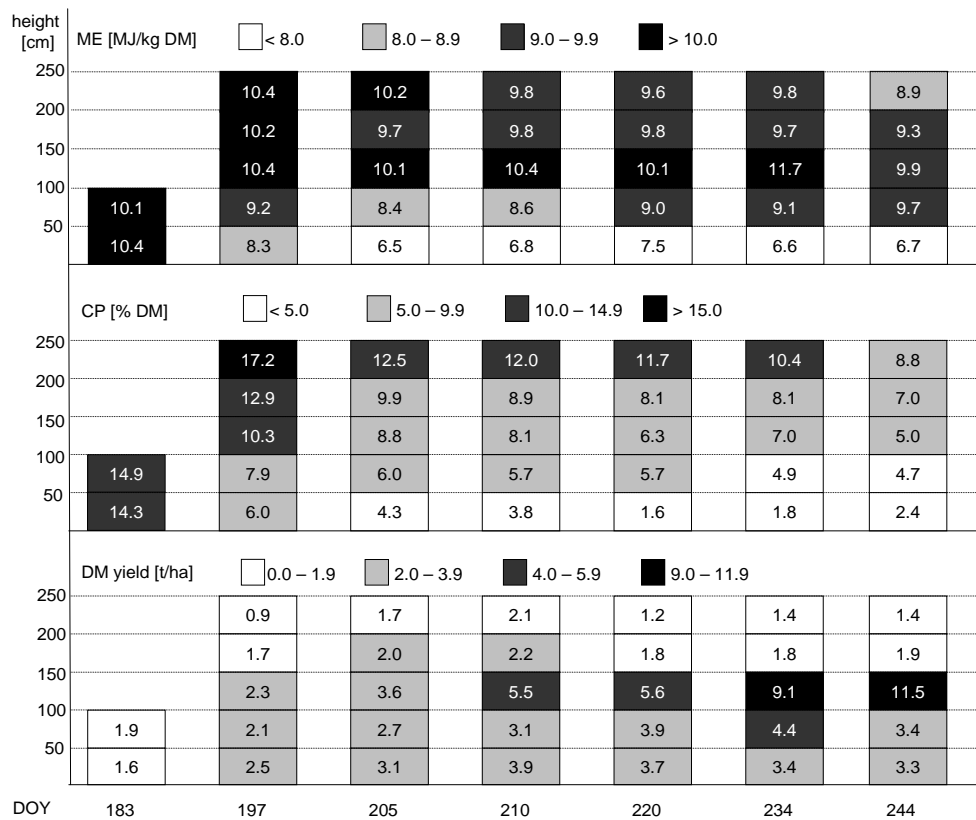


Figure 6.2: Mean segmental content of ME, CP and DM yield in maize plants for each measurement date in 2008. Plant material higher than 250 cm was included in segment height 200 – 250 cm for reference analysis.

sensitive indicator of vegetation (Jackson, 1983) and effective in normalizing irradiance conditions (Tucker, 1977) and, thus, was considered appropriate to characterize spectra. Both angle and height were significant as main effects, whereas the interaction was not (Table 6.2). However, mathematical procedures during calibration development were not regarded in this analysis. Yet, mathematical treatments may cause differences in prediction accuracy among individual angle/height combinations. Thus, examination of every single combination of angle

Table 6.2: Effect of angle and height and the interaction angle x height on reflectance, expressed by the Simple Ratio (SR) vegetation index.

Effect	DF	SS	MS	F	P
angle	2	372.2	186.1	4.3	0.0139
height	4	3437.9	859.5	19.9	<.0001
angle x height	8	557.7	69.7	1.6	0.1178

and height is necessary in order to identify best prediction accuracies for the target variables.

### 6.3.3 Prediction of DM yield, CP and ME in total biomass as related to angle and height

#### Three-Sensor strategy (S3-Scenario)

Three-Sensor strategy (S3-scenario, where S stands for sensor) comprises the identification of such angle and height combinations which allow the best prediction accuracy for DM yield, CP and ME in total biomass, respectively (Table 6.3). Angle/height adjustments ( $90^\circ$ , 0 – 50 cm), scatter correction and math treatment

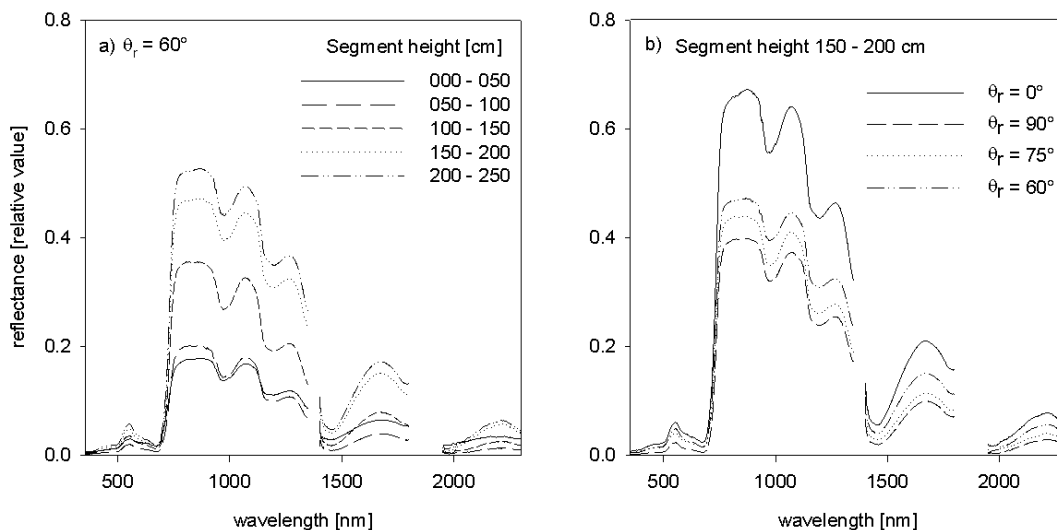


Figure 6.3: Relative reflectance depending on a) segment height and b) zenith view angle adjustments. Spectra are exempt from water absorption bands at 1400 nm and 1900 nm.

are similar for DM yield regarding the entire (355 – 2300 nm) and reduced (620 – 1000 nm) wavelength range in order to achieve best prediction accuracies. SECVs of <2.2 t DM/ha suggest that spectral signatures of biomass in the bottom layer of

the stand are closely related to the total crop biomass. The same accounts for CP, whereas for ME differences in height, scatter correction and math treatment occur between the entire and reduced wavelength range (Table 6.3). Unlike to DM

Table 6.3: Statistics of the cross-validation (CV) for DM yield (DM) [t/ha], crude protein (CP) [% DM] and metabolisable energy (ME) [MJ/kg DM] of the total crop biomass. Shown are these height and angle combinations for which SECV was lowest in the entire (355 – 2300 nm) and reduced (620 – 1000 nm) wavelength range.

constituent	n	angle	height	scatter correction	math treatment	SECV	RSQ <sub>CV</sub>	RSC
entire wavelength range (355 – 2300 nm)								
DM	33	90	000-050	MSC	1 10 10	2.2	0.86	2.7
CP	30	60	150-200	MSC	1 10 10	0.6	0.76	2.0
ME	27	75	200-250	SNV-D	2 10 10	0.3	0.89	3.0
reduced wavelength range (620 – 1000 nm)								
DM	32	90	000-050	MSC	0 10 10	1.7	0.92	3.6
CP	28	60	150-200	MSC	1 8 8	0.4	0.90	3.2
ME	28	75	100-150	MSC	1 6 6	0.3	0.89	3.0

n: number of samples; angle: zenith view angle in degree (°); height: plant segment above ground in cm; SECV: standard errors of cross-validation; RSQ<sub>CV</sub>: coefficient of determination of the cross validation; RSC: stability factor, ratio of standard deviation and SECV.

yield, spectral information for total crop quality seems to be available in the intermediate (100 – 150 cm) and upper (200 – 250 cm) layers of the crop. However, prediction accuracy is improved for DM yield and CP regarding SECV, RSQ<sub>CV</sub> and RSC in the reduced wavelength range, whereas prediction accuracy for ME remains constant which may be due to the high amount of noise in longer wavelength regions.

### Development of one-sensor applications (S1-scenario)

Application of the S3-scenario would require three sensors measuring the reflectance in different heights and with different angles. In order to reduce the technical effort a restriction in the number of sensors to only one would be desirable (S1-scenario). On the one hand, this would certainly result in maximum accuracy for the first parameter to be chosen (main target variable), on the other hand a loss of accuracy could possibly occur for one or both other constituents. The first question to respond to is to what extent the prediction accuracy for these two constituents changes when one constituent is chosen as main target variable. Reference

data for this are the accuracies determined in the S3-scenario above (Table 6.3) and settings for angle and height are fixed at the same level as in the measurement for the main target variable using best math treatments possible for this angle/height combination (Table 6.4). Regarding the entire wavelength range reduction in accuracy occurs in the range of 0.1 to 0.5. In contrast, in the reduced wavelength range reduction ranges between 0.1 and 0.6 which is due to a generally increased level of RSC reference values compared to the entire wavelength range, so that even accuracy levels in a lower but still acceptable range mark relatively high reductions. Hence, a direct comparison of entire and reduced wavelength ranges is not sensible.

It is of further interest which constituent should be chosen as main target variable in order to induce lowest reduction in accuracy in the two other constituents. By ranking all statistical parameters, ME proves as the appropriate main target variable in the entire wavelength range, where losses in accuracy for DM and CP are lowest with 0.3 and 0.1, respectively, compared to values of the S3-scenario. In the reduced wavelength range highest overall accuracies can be found with DM yield as main target variable, with losses in accuracy for CP and ME of 0.4 and 0.2, respectively.

#### **6.3.4 Comparison of nadir and off-nadir measurements**

Regarding nadir measurements prediction accuracy for DM yield and CP is slightly improved in the reduced (620 – 1000 nm) wavelength range compared to the entire (355 – 2300 nm) wavelength range, whereas prediction accuracy for ME remains constant (Table 6.5). These results generally correspond well with off-nadir measurement, but improvements are less pronounced.

In contrast, the comparison of nadir and off-nadir measurements shows distinctive differences in prediction accuracies for DM yield, CP and ME. Prediction accuracy for DM yield using off-nadir measurements is improved by up to 0.6 and for ME by up to 0.4 in the entire and reduced wavelength range, respectively. In former studies, prediction accuracy for DM yield or related parameters (e.g. stand density) was reported with RSQ values between 0.57 and 0.79 (Senay *et al.*, 2000; Freeman *et al.*, 2007; Thorp *et al.*, 2008; Bausch *et al.* 2008; Salazar *et al.*, 2008)



Table 6.4: Calibration statistics of S1-scenario, when angle and height are adopted from the main target variable as determined in the S3-scenario for the entire (355 – 2300 nm) and reduced (620 – 1000 nm) wavelength range.

entire wavelength range (355 – 2300 nm)												
	SECV	RSQ <sub>cv</sub>	RSC	reduction	SECV	RSQ <sub>cv</sub>	RSC	reduction	SECV	RSQ <sub>cv</sub>	RSC	reduction
DM	2.2	0.86	2.7	-	3.2	0.48	1.4	0.5	2.5	0.73	1.9	0.3
CP	1.2	0.72	1.8	0.1	0.6	0.76	2.0	-	0.7	0.67	1.7	0.1
ME	0.5	0.67	1.7	0.4	0.4	0.83	2.4	0.2	0.3	0.89	3.0	-
reduced wavelength range (620 – 1000 nm)												
	SECV	RSQ <sub>cv</sub>	RSC	reduction	SECV	RSQ <sub>cv</sub>	RSC	reduction	SECV	RSQ <sub>cv</sub>	RSC	reduction
DM	1.7	0.92	3.6	-	3.2	0.53	1.5	0.6	2.9	0.64	1.6	0.6
CP	1.1	0.75	2.0	0.4	0.4	0.90	3.2	-	0.7	0.73	1.9	0.4
ME	0.4	0.82	2.3	0.2	0.3	0.86	2.6	0.1	0.3	0.89	3.0	-

SECV: standard errors of cross-validation; RSQ<sub>cv</sub>: coefficient of determination of the cross validation; RSC: stability factor, ratio of standard deviation and SECV; reduction: relative reduction in RSC as compared to the RSC value in the S3-scenario. Fields highlighted grey show the calibration statistics of the main target variable from the S3-scenario.

generally using VIs from top reflectance measurements. Dos Santos Simões *et al.* (2005) got a wide range of RSQ values (0.28 to 0.98) for DM yield in sugar cane using different VIs and correlated wavelength bands. However, Gianelle and Guastella (2007) reported improved results for the determination of biomass using VIs based on off-nadir measurements, resulting in a RSQ value of 0.81 compared to 0.77 (nadir). Although literature data correspond well with the results from nadir measurements found in this study, the level of accuracy from measurements conducted inside the canopy with the reduced wavelength range outyields those results by far (RSQ<sub>cv</sub> of 0.92, RSC of 3.6). The bottom layer (0 to 50 cm above soil) is the segment with the highest soil interference although a zenith view angle of 90° minimizes this impact. Spectra of this part of the plant show a wide deviation compared to upper plant segments and lighting conditions are characterised by low incoming radiance, strong shading effects and hence a reduced reflectance (Figure 6.3). However, this part of the plant has only few large, dark green leaves and thick stalk elements. This might result in distinctive reflectance features, especially in the visible and near infrared region, which are known as highly correlated to biomass (Cho *et al.*, 2007; Biewer *et al.*, 2009a).

Top reflectance measurements generally show good prediction accuracy for CP or related parameters such as chlorophyll content or nitrogen uptake using VIs (Daughtry *et al.*, 2000; Elwadie *et al.*, 2005; Miao *et al.*, 2009). This might be related to the high content of proteins in the upper plant leaves where optimal light conditions and maximum rates of photosynthesis occur, which results in high reflectance and hence good prediction accuracies (Charles-Edwards *et al.*, 1987; Lemaire and Gastal, 1997). The coefficients of determination obtained by nadir measurements in the present study (Table 6.5) correlate well to these former findings and can hardly be reached using off-nadir measurements inside the canopy. One reason for the relative poor results may be that off-nadir measurements only covered a plant height of 250 cm due to technical limitations and hence, panicles and top leaves with high CP concentration were not included, whereas the reference value referred to the top of the plant from 200 cm upwards. Recording these segments separately might enhance the determination for CP. However, CP can be determined with an RSQ<sub>cv</sub> value of 0.90 for theS3-scenario and, still, with an

$RSQ_{cv}$  of 0.75 in the S1-scenario regarding the reduced wavelength range (Table 6.3 and 6.4). The latter prediction accuracy equals to a reduction of 0.4 compared to nadir measurements, but is still higher than in related research studies (e.g. Freeman *et al.*, 2007; Schmidt *et al.*, 2009).

Table 6.5: Statistics of the cross-validation (CV) for DM yield (DM) [t/ha], crude protein (CP) [% DM] and metabolisable energy (ME) [MJ/kg DM] of nadir measurements for the entire (355- 2300 nm) and reduced (620 - 1000 nm) wavelength range and relative reduction in RSC with off-nadir measurements compared to nadir measurements.

nadir							RSC reduction with off-nadir compared to nadir	
entire wavelength range (355 – 2300 nm)								
	n	scatter correction	math treatment	SECV	$RSQ_{cv}$	RSC	S3-scenario	S1-scenario
DM	34	MSC	1 10 10	2.6	0.79	2.2	-0.2	0.1
CP	32	none	2 6 6	0.9	0.90	3.2	0.4	0.5
ME	34	none	1 10 10	0.4	0.81	2.1	-0.4	-0.4
reduced wavelength range (620 – 1000 nm)								
DM	33	none	0 10 10	2.6	0.81	2.2	-0.6	-0.6
CP	32	none	2 4 4	0.8	0.92	3.4	0.1	0.4
ME	32	MSC	2 4 4	0.4	0.78	2.1	-0.4	-0.1

n: number of samples; SECV: standard errors of cross-validation;  $RSQ_{cv}$ : coefficient of determination of the cross validation; RSC: stability factor, ratio of standard deviation and SECV; RSC reduction: relative reduction in RSC as compared to the RSC value in the S3- and S1-scenario.

Metabolisable energy can be adequately determined using laboratory near infrared reflectance spectroscopy (e.g. DeBoever *et al.*, 1995; Castrillo *et al.*, 2005). However, an online detection of ME directly in the field would save time and costs otherwise needed for sample preparation. Off-nadir measurements in the present study show very good prediction accuracy in the reduced wavelength range with  $RSQ_{cv}$  values of 0.89 and 0.82 for the S3-Scenario and S1-scenario, respectively. These results exceed nadir measurements by up to 0.4 (Table 6.5) and are comparable to laboratory values (DeBoever *et al.*, 1997, Castrillo *et al.*, 2005).

It should be pointed out that the reference data were determined by laboratory NIRS and, hence, incorporated prediction errors by themselves. Thus, the results reported in the present study indicate the lower boundaries of the spectral methodology and may be further improved using reference values determined chemi-

cally in the laboratory. Furthermore, the use of an additional sensor that measures incoming radiation in order to adjust the reflectance signal to changing light conditions or the application of artificial light to obtain stable measurements which are free of weather interferences may still enhance the precision of prediction models.

#### **6.4 Conclusions**

This study was conducted to explore the potential of off-nadir field spectral measurements inside a maize canopy with different angle/height adjustments of the sensor in order to predict DM yield, CP and ME in total biomass. The following conclusions can be drawn from this three years lasting experiment:

- (i) Spectral response is significantly dependent on height and angle adjustments due to the complex relationship of light and shade contribution inside a canopy, distribution of constituents and sensor view geometry.
- (ii) Prediction of DM yield, CP and ME in total biomass is possible with field spectroscopic measurements conducted inside the canopy. Results are improved for the reduced wavelength range (620 – 1000 nm) compared to the entire wavelength range (355 – 2300 nm). Maximum  $RSQ_{cv}$  values are between 0.89 (ME) and 0.92 (DM yield) in the reduced wavelength range.
- (iii) In comparison with nadir measurements, off-nadir measurements resulted in improved accuracies for DM yield and ME, whereas prediction accuracy for CP obtained by nadir measurements can hardly be reached by off-nadir adjustments.

## 7 General discussion

The objectives of this study were to evaluate quantitative spectroscopic analysis methods with a focus on possibilities of technical and analytical enhancements, respectively. Therefore a laboratory study was carried out with press cakes provided by the Integrated Generation of Solid Fuels and Biogas from Biomass (IFBB-System), that provides a highly digestible liquid component (press fluid) and a solid fuel (press cake) by mechanically dehydration of silages. The press cakes were characterised by heterogeneous parent materials due to the wide range of silages used in the related studies (Reulein *et al.*, 2007; Wachendorf *et al.*, 2009). In addition, two field experiments were conducted to examine the impact of clouds on field spectroscopic measurements as well as to explore the potential of off-nadir measurements inside a canopy characterised by distinct crop heights.

Both, laboratory and field spectroscopic measurements, has been proven as an useful tool for the detection of biochemical and biophysical parameters (Park *et al.*, 1998; Mutanga *et al.*, 2003; Cozzolino *et al.*, 2006; Jain *et al.*, 2007). However, laboratory technology often is recommended for homogeneous sample compositions, and field spectroscopic measurements are limited due to environmental impacts during data collection such as passing clouds, wind, canopy background, and changing solar altitude.

Although field spectroscopy is carried out under field conditions, this method has the advantage of no sample preparation and agronomists are able to record directly important plant and quality parameters during crop management on the field. This reduces costs, labour, and time and can provide a versatile tool for online quality assessment, particularly in cropping systems for energetic purposes. Hence, the challenge of analysis of data collected under field conditions is to minimize negative effects interfering with reflection signals as well as to identify spectral regions closely correlated to the target variable in question (Biewer, 2009). In this context it is sensible to include all spectral information available, since field spectroscopic studies conducted over grassland (Biewer *et al.*, 2009a, b) prove best results applying hyperspectral analysis. However, practical use might be limited due to high technical effort for data collection in the whole visi-

ble and near infrared range (350 – 2500 nm). The application of a reduced wavelength range (620 – 1000 nm), as tested in this study, still provides sufficient spectral information in combination with reduced technical input. This advances practical application for on-the-go solutions.

Other important aspects in field spectroscopic applicability for potential on-the-go solutions are the mounting and adjustment of the sensor on a tractor. For low growing crops, such as cereals, the sensor is mounted on top of the tractor, measuring bidirectionally top-of-canopy reflectance (Heege *et al.*, 2008). However, for energy crops with plant heights of more than three meters this mounting becomes difficult. Furthermore, it is questioned to what extent top-of-canopy reflectance is able to predict quality parameters. Our study shows that prediction accuracy is reduced for DM yield and ME in total biomass using top-of-canopy reflectance. In contrast, these target variables can be predicted very well using off-nadir measurements collected inside the canopy. This would enable a mounting of the sensor sideways on the tractor in a distinct measurement height and with a distinct zenith view angle depending of the required main target variable.

The great dependency on weather conditions is probably the most limiting factor for practical implementation regarding agronomic purposes and requires solutions in order to reduce these environmental impacts. A widely practised method is the use of an additional sensor that measures the incoming radiation to adjust the reflectance signal to changing light conditions (Reusch, 2005; Larsolle and Hamid Muhammed, 2007). Another approach, tested in this study, is aimed at the enlargement of the calibration basis by including all possible degrees of sky cover. Although this approach shows very good results, it is questioned if a sufficient large basis of data can be collected under changing degrees of sky cover to obtain a robust and stable calibration equation, since atmospheric conditions are highly variable in space and time and, hence, irradiance conditions change permanently.

This suggests that the potential of field spectroscopy is not fully exploited, yet, and further research is still needed to evaluate these methods by effects of varying sites and vegetation periods in order to enhance the robustness and portability of

models to other environmental conditions and in order to facilitate practical implementation in agricultural cropping systems.

## 8 Conclusions

The following conclusions can be drawn from the laboratory study and the two field experiments:

- i) The concentration of major constituents relevant for combustion, such as N, K, ash, and CF can be predicted with satisfactory accuracy in heterogeneous composed press cakes. Chloride and P still can be predicted with moderate accuracy. Mass flows of major organic and mineral constituents during mechanical separation based on NIR-predicted values can be assessed with appropriate accuracy (RSQ 0.72 – 0.99).
- ii) The impact of clouds on reflectance signals is evident due to a reduction of prediction accuracy of DM yield with increasing degree of sky cover. Nevertheless, overall calibrations, comprising data recorded under a wide range of simulated degrees of sky cover, showed very good results for DM, CP, ash and ME (RSQ 0.86 – 0.94).
- iii) Spectral response obtained by off-nadir measurements inside a maize canopy is significantly dependent on height and angle adjustments. Nevertheless, prediction of DM yield, CP and ME of the whole crop shows very good accuracies (RSQ 0.89 – 0.92) and partly exceed results obtained by nadir data collection.

The results of this study have shown the potential of laboratory and field spectroscopy and proved its usefulness for predicting DM yield, nutrition constituents as well as mineral composition in a wide range of different crops. Prediction accuracies determined with field spectroscopic data generally were in line with results reported in laboratory studies. Nevertheless, further research is needed to validate first findings regarding effects of changing weather conditions presented in this study and to enhance on-the-go applications using sideways measurements inside high growing canopies.



## 9 Summary

A real-time analysis of renewable energy sources, such as arable crops, is of great importance with regard to an optimised process management, since aspects of ecology and biodiversity are considered in crop production in order to provide a sustainable energy supply by biomass.

This study was undertaken to explore the potential of spectroscopic measurement procedures for the prediction of potassium (K), chloride (Cl), and phosphate (P), of dry matter (DM) yield, metabolisable energy (ME), ash and crude fibre contents (ash, CF), crude lipid (EE), nitrate free extracts (NfE) as well as of crude protein (CP) and nitrogen (N), respectively in pre-treated samples and undisturbed crops.

Three experiments were conducted, one in a laboratory using near infrared reflectance spectroscopy (NIRS) and two field spectroscopic experiments.

Laboratory NIRS measurements were conducted to evaluate to what extent a prediction of quality parameters is possible examining press cakes characterised by a wide heterogeneity of their parent material. 210 samples were analysed subsequent to a mechanical dehydration using a screw press. Press cakes serve as solid fuel for thermal conversion.

Field spectroscopic measurements were carried out with regard to further technical development using different field grown crops.

A one year lasting experiment over a binary mixture of grass and red clover examined the impact of different degrees of sky cover on prediction accuracies of distinct plant parameters. Furthermore, an artificial light source was used in order to evaluate to what extent such a light source is able to minimise cloud effects on prediction accuracies.

A three years lasting experiment with maize was conducted in order to evaluate the potential of off-nadir measurements inside a canopy to predict different quality parameters in total biomass and DM yield using one sensor for a potential on-the-go application. This approach implements a measurement of the plants in 50

cm segments, since a sensor adjusted sideways is not able to record the entire plant height. Calibration results obtained by nadir top-of-canopy reflectance measurements were compared to calibration results obtained by off-nadir measurements.

Results of all experiments approve the applicability of spectroscopic measurements for the prediction of distinct biophysical and biochemical parameters in the laboratory and under field conditions, respectively. The estimation of parameters could be conducted to a great extent with high accuracy. An enhanced basis of calibration for the laboratory study and the first field experiment (grass/clover-mixture) yields in improved robustness of calibration models and allows for an extended application of spectroscopic measurement techniques, even under varying conditions. Furthermore, off-nadir measurements inside a canopy yield in higher prediction accuracies, particularly for crops characterised by distinct height increment as observed for maize.

## 10 Zusammenfassung

Für die Bereitstellung biogener Energieträger ist eine möglichst zeitnahe Erfassung ausgewählter Qualitätsparameter von entscheidender Bedeutung. Diese rückt umso stärker in den Fokus als auch ökologische und biodiversitäre Aspekte bei der Pflanzenproduktion Berücksichtigung finden, um eine möglichst nachhaltige Energieversorgung durch Biomasse zu gewährleisten.

Die vorliegende Untersuchung evaluiert das Potenzial spektroskopischer Messverfahren zur Erfassung von Kalium (K), Chlorid (Cl) und Phosphat (P), des Trockenmasseertrags (TM-Ertrag), der metabolisierbaren Energie (ME), des Aschegehaltes (Asche), des Rohfasergehaltes (RF), des Rohfetts (RL), nitratfreier Extraktstoffe (NfE) und des Rohproteins (RP) bzw. Stickstoffs (N) in aufbereiteten Proben und am ungestörten Pflanzenbestand.

Dazu wurden eine laborspektroskopische und zwei feldspektroskopische Untersuchungen durchgeführt.

Die laborspektroskopischen Messungen (NIRS) dienen zur Klärung inwieweit eine Qualitätsbestimmung an Presskuchen aus dem Zweikulturen-Nutzungssystem und extensiv genutzter Grünlandbestände möglich ist. Die insgesamt 210 Proben sind durch sehr heterogenes Ausgangsmaterial gekennzeichnet, die im Rahmen des IFBB-Verfahrens mechanisch entwässert und anschließend getrocknet wurden. Die Presskuchen dienen in pelletierter Form als thermischer Festbrennstoff.

Die feldspektroskopischen Messungen wurden unter dem Aspekt der Verfahrensentwicklung an unterschiedlichen Freilandbeständen durchgeführt.

Ein einjähriger Versuch im Klee gras diente der Prüfung des Einflusses unterschiedlicher Bewölkungsgrade auf die Vorhersagegenauigkeit bestimmter Pflanzenparameter. Zudem wurde untersucht, inwieweit der Einsatz einer künstlichen Lichtquelle dem Einfluss von Wolken auf die Vorhersagegenauigkeit entgegen wirken kann.

Ein dreijähriger Versuch im Mais sollte den Einsatz seitlicher, innerhalb des Bestandes durchgeführter spektroskopischer Messungen evaluieren, um eine mög-

lichst hohe Vorhersagegenauigkeit ausgewählter Pflanzenparameter mittels eines Sensors zu erzielen. Kalibrationsergebnisse senkrechter Messungen wurden diesem Ansatz gegenübergestellt.

Die Ergebnisse der vorliegenden Untersuchungen bestätigen die Eignung spektroskopischer Messungen für die Bestimmung ausgewählter Pflanzenparameter, sowohl im Labor als auch unter Feldbedingungen. Die Vorhersage der Parameter erfolgte in allen Untersuchungen weitestgehend mit sehr hoher Güte. Die erweiterte Kalibrationsgrundlage im Labor- und ersten Feldversuch (Klee gras) zeigt eine Verbesserung der Robustheit von Kalibrationsmodellen und ermöglicht somit erweiterte Einsatzmöglichkeiten des jeweiligen Verfahrens, auch unter sich ändernden Umweltbedingungen. Zudem wird deutlich, dass mithilfe seitlicher Messungen innerhalb eines Pflanzenbestandes höhere Schätzgenauigkeiten erreicht werden können, insbesondere dann, wenn die Bestände durch ausgeprägtes Höhenwachstum gekennzeichnet sind wie dies beim Mais der Fall ist.

---

## 11 References

- Amon T., *et al.*, 2007: Biogas production from maize and dairy cattle manure — influence of biomass composition on the methane yield. *Agric Ecosyst Environ* 118:173–182.
- Andrés S., *et al.*, 2005: Nutritive evaluation of herbage from permanent meadows by near-infrared reflectance spectroscopy: 1. Prediction of chemical composition and *in vitro* digestibility. *J Sci Food Agric* 85:1564–1571.
- Asner, G.P., *et al.*, 1998: Ecological research needs from multiangle remote sensing data. *Remote Sensing of Environment* 63, 155–165.
- Azzouz T., *et al.*, 2003: Comparison between different data pre-treatment methods in the analysis of forage samples using near-infrared diffuse reflectance spectroscopy and partial least-squares multivariate calibration method. *Anal Chim Acta* 484:121–134.
- Barnes R.J., *et al.*, 1989: Standard normal variate transformation and de-trending of near-infrared diffuse reflectance spectra. *Appl Spectrosc* 43(5):772–777.
- Bauer, M.E., 1985: Spectral Inputs to Crop Identification and Condition Assessment. *Proceedings of the IEEE* 73 (6), 1071–1085.
- Bausch, W.C., *et al.*, 2008: Quickbird satellite and ground-based multispectral data correlations with agronomic parameters of irrigated maize grown in small plots. *Biosystems Engineering* 101: 306–315.
- Berardo N., *et al.*, 1997: Near infrared calibration of chemical constituents of *Cajanus cajan* (pigeon pea) used as forage. *Anim Feed Sci Technol* 69:201–206.
- Berg, H., 1948: Beziehungen zwischen Globalstrahlung, Sonnenscheindauer und Bewölkung. *Pure and Applied Geophysics* 13 (5-6), 157–166.

- Biewer, S., 2009: Hyperspectral field measurements to determine dry matter yield and nutritive value of legume-grass swards. Doctoral thesis, Witzenhäusen, Germany.
- Biewer, S., *et al.*, 2009a: Prediction of yield and the contribution of legumes in legume-grass mixtures using field spectrometry. *Precision Agriculture* 10: 128–144.
- Biewer S., *et al.*, 2009b: Determination of Dry Matter Yield from Legume-Grass Swards by Field Spectroscopy. *Crop Sci* 49: 1927–1936.
- Biewer S., *et al.*, 2009c: Development of canopy reflectance models to predict forage quality of legume-grass mixtures. *Crop Sci* 49:1917–1926.
- Broge, N.H. and Leblanc, E., 2000: Comparing prediction power and stability of broadband and hyperspectral vegetation indices for estimation of green leaf area index and canopy chlorophyll density. *Remote Sensing of Environment* 76, 156–172.
- Brunet D., *et al.*, 2007: Determination of carbon and nitrogen contents in Alfisols, Oxisols and Ultisols from Africa and Brazil using NIRS analysis: effects of sample grinding and set heterogeneity. *Geoderma* 139:106–117.
- Castrillo C., *et al.*, 2005: Energy evaluation of extruded compound foods for dogs by near-infrared spectroscopy. *J Anim Physiol Anim Nutr* 89:194–198.
- Charles-Edwards, D.A. *et al.*, 1987: An analysis of spatial variation in the nitrogen content of leaves from different horizons within a canopy. *Annals of Botany* 60, 421–426.
- Cho, M.A., *et al.*, 2007: Estimation of green/herb biomass from airborne hyperspectral imagery using spectral indices and partial least squares regression. *International Journal of Applied Earth Observation and Geoinformation* 9: 414–424.
- Clark, R.N., 1999: Spectroscopy of rocks and minerals and principles of spectroscopy. In: Rencz, A. N. (ed.): *Remote Sensing for the Earth Sciences: Manual of Remote Sensing* (pp. 3-58). 3. ed., Wiley, New York, USA.

- Cozzolino D. and Morón, A., 2004: Exploring the use of near infrared reflectance spectroscopy (NIRS) to predict trace minerals in legumes. *Anim Feed Sci Technol* 111:161–173.
- Cozzolino, D., *et al.*, 2006: Measurement of chemical composition in wet whole maize silage by visible and near infrared reflectance spectroscopy. *Animal Feed Science and Technology* 129: 329–336 .
- Curran, P.J., 1983: Estimating green LAI from multispectral aerial photography. *Photogrammetric Engineering and Remote Sensing* 49: 1709–1720 .
- Curtiss, B. and Goetz, A.F.H., 1999: Field spectrometry: Techniques and instrumentation. In: Hatchell, D.C. (Ed), *ASD Technical Guide*. Boulder, USA, pp. 73–82.
- Daughtry, C.S.T. *et al.*, 2000: Estimating Corn Leaf Chlorophyll Concentration from Leaf and Canopy Reflectance. *Remote Sensing of Environment* 74, 229–239.
- Daughtry, C.S.T., *et al.*, 2006: Remote sensing of crop residue cover and soil tillage intensity. *Soil & Tillage Research* 91, 101–108.
- Deaville E.R. and Givens, D.I., 1998: Regions of normalised near infrared reflectance difference spectra related to the rumen degradation of fresh grass, grass silage and maize silage. *Anim Feed Sci Technol* 72:41–51.
- DeBoever, J.L. *et al.*, 1995: The use of NIRS to predict the chemical composition and the energy value of compound feeds for cattle. *Animal Feed Science Technology* 51, 243–253.
- DeBoever, J.L., *et al.*, 1996: Prediction of the feeding value of grass silages by chemical parameters, *in vitro* digestibility and near-infrared reflectance spectroscopy. *Animal Feed Science Technology* 60: 103–115.
- DeBoever J.L., *et al.*, 1997: Prediction of the feeding value of maize silages by chemical parameters, *in vitro* digestibility and NIRS. *Anim Feed Sci Technol* 66:211–222.

- Dos Santos Simões, M. *et al.*, 2005: Spectral variables, growth analysis and yield of sugarcane. *Sci. Agric.* 62 (3), 199–207.
- El Hajj, M., *et al.*, 2008: Relative Radiometric Normalization and Atmospheric Correction of a SPOT 5 Time Series. *Sensors* 8, 2774–2791.
- Elwadie, M.E. *et al.*, 2005: Remote Sensing of Canopy Dynamics and Biophysical Variables Estimation of Corn in Michigan. *Agronomy Journal* 97, 99–105.
- Erasmi, S. and Kappas, M., 2003: Determination of crop stress using spectral transformations of Hyperspectral data. In: Habermeyer, M., Müller, A. & S. Holzwarth (eds.): 3rd EARSeL Workshop on Imaging Spectroscopy. 13-16 May 2003, Herrsching, Germany, S. 496-503 (ISBN 2-908885-26-3).
- Erasmi, S. and E.S. Dobers. 2004: Potential and limitations of spectral reflectance measurements for the estimation of the site specific variability in crops. p. 42-51). *In: M. Owe and G. D'Urso (Eds.) Remote Sensing for Agriculture, Ecosystems and Hydrology V. Proc. of SPIE Vol. 5232. Barcelona, Spain. 8. Sept. 2003. Bellingham, WA USA.*
- Feister, U. and Shields, J., 2005: Cloud and radiance measurements with the VIS/NIR Daylight Whole Sky Imager at Lindenberg (Germany). *Meteorologische Zeitschrift* 14 (5), 627–639.
- Fitzgerald, G.J., *et al.*, 2006: Spectral and thermal sensing for nitrogen and water status in rainfed and irrigated wheat environments. *Precision Agriculture* 7: 233–248.
- Foley W.J., *et al.*, 1998: Ecological applications of near infrared reflectance spectroscopy—a tool for rapid, cost-effective prediction of the composition of plant and animal tissues and aspects of animal performance. *Oecologia* 116:293–305.
- Freeman, K.W. *et al.*, 2007: By-Plant Prediction of Corn Forage Biomass and Nitrogen Uptake at Various Growth Stages Using Remote Sensing and Plant Height. *Agronomy Journal* 99, 530–536.



- Friedl, M.A., *et al.*, 1994. Estimating grassland biomass and leaf area index using ground and satellite data. *International Journal of Remote Sensing* 15: 1401–1420.
- Gastal, F. and Lemaire, G. 2002: N uptake and distribution in crops: an agronomical and ecophysiological perspective. *Journal of Experimental Botany*, Vol. 53 (370), 789–799.
- Gausmann, H.W., *et al.*, 1969: Reflectance of cotton leaves and their structure. *Remote Sensing of Environment* 1: 19-22.
- Geladi, P. and Kowalski, B.R., 1986: Partial least-squares regression: a tutorial. *Analytica Chimica Acta* 185: 1–17.
- Gianelle, D. and Guastella, F. 2007: Nadir and off-nadir hyperspectral field data: strengths and limitations in estimating grassland biophysical characteristics. *International Journal of Remote Sensing* 28: 1547–1560.
- Gesellschaft für Ernährungsphysiologie (GfE), 1995: Energie und Nährstoffbedarf landwirtschaftlicher Nutztiere Nr. 6. Empfehlungen zur Energie- und Nährstoffversorgung der Mastrinder (Energy and nutritional requirement of agricultural livestock No 6. Recommendations for energy and nutrient supplies of feeder cattle). DLG-Verlag, Frankfurt a.M.
- Goel, P.K. *et al.*, 2003: Potential of airborne hyperspectral remote sensing to detect nitrogen deficiency and weed infestation in corn. *Computers and Electronics in Agriculture* 38, 99–124.
- González-Martín I, *et al.*, 2007: Use of NIRS technology with a remote reflectance fibreoptic probe for predicting mineral composition (Ca, K, P, Fe, Mn, Na, Zn), protein and moisture in alfalfa. *Anal Bioanal Chem* 387:2199–2205.
- Graß R., *et al.*, 2009: Die integrierte Biogas- und Festbrennstoffherzeugung aus Ganzpflanzensilagen (Integrated biogas and solid fuel production from whole-crop silage). *Berichte Landwirtschaft* 87:43–64
- Greenwood, D.J. *et al.*, 1990: Decline in Percentage N of C3 and C4 Crops with Increasing Plant Mass. *Annals of Botany* 66, 425–436.

- Greul U., 1998: VDI-Fortschrittsberichte, Reihe 6: Energietechnik, Nr. 388, Experimentelle Untersuchung feuerungstechnischer NO<sub>x</sub>-Minderungsverfahren bei der Kohlenstaubverbrennung (VDI Progress reports, series 6: Energy technique, Nr. 388, Experimental investigation on NO<sub>x</sub> mitigation techniques for the combustion of carbon dust), Düsseldorf, Germany: VDI-Verlag.
- Griffith, J.A., *et al.*, 2001: A multivariate analysis of biophysical parameters of tallgrass prairie among land management practices and years. *Environmental Monitoring and Assessment* 68, 249–271.
- Govender, M., *et al.*, 2008: A comparison of satellite hyperspectral and multispectral remote sensing imagery for improved classification and mapping of vegetation. *Water SA* 34 (2), 147–154.
- Günzler, H. and Gremlich, H.-U., 2003: IR-Spektroskopie. Eine Einführung. Wiley-VCH, Weinheim, Germany.
- Halgerson J.L., *et al.*, 2004: Near-infrared reflectance spectroscopy prediction of leaf and mineral concentrations in Alfalfa. *Agron J* 96:344–351.
- Hansen, P.M. and Schjoerring, J.K., 2003: Reflectance measurement of canopy biomass and nitrogen status in wheat crops using normalized difference vegetation indices and partial least squares regression. *Remote Sensing of Environment* 86: 542–553.
- Hartmann, H., 2001: Brennstoffzusammensetzung und –eigenschaften (Composition and characteristics of fuels). In: Kaltschmitt M, Hartmann H (eds) *Energie aus Biomasse: Grundlagen. Techniken und Verfahren*. Springer-Verlag, Berlin, Heidelberg, New York, pp 248–272.
- Hasenfratz, E., 2006: Die Rolle der Globalstrahlung im Klimasystem Südwestdeutschlands - Vergleichende statistische Untersuchungen zu ihrer räumlichen Variabilität. Doctoral thesis, University of Mainz, Germany.
- Hatchell, D.C. (Ed), 1999: *ASD Technical Guide*. Boulder, USA.

- Heege, H.J., *et al.*, 2008: Prospects and results for optical systems for site-specific on-the-go control of nitrogen-top-dressing in Germany. *Precision Agriculture* 9: 115–131.
- Herrmann C, *et al.*, 2007: Parameters influencing substrate quality and biogas yield. In: Proceedings of the 15<sup>th</sup> European Biomass Conference and Exhibition, Berlin, Germany, 2007, pp 809–819. Florence, Italy, ETA-Renewable Energies.
- Hildebrandt, G., 1996: Fernerkundung und Luftbildmessung: für Forstwirtschaft, Vegetationskartierung und Landschaftsökologie. Wichmann, Heidelberg, Germany.
- Huete, A.R. and Jackson, R.D., 1988: Soil and atmosphere influences on the spectra of partial canopies. *Remote Sensing of Environment* 25 (1): 89–105.
- Jackson, R.D. and Pinter, P.J., 1986: Spectral Response of Architecturally Different Wheat Canopies. *Remote Sensing of Environment* 20, 43–56.
- Jain, N., *et al.*, 2007: Use of hyperspectral data to assess the effects of different nitrogen applications on a potato crop. *Precision Agriculture* 8: 225–239.
- Jensen, J.R., 2000: Remote sensing of the environment: An earth resource perspective. Prentice Hall, Upper Saddle River, New Jersey, USA.
- Kneizys, F.X., *et al.*, 1988: Atmospheric transmittance/radiance: Computer code LOW TRAN-7, Air Force Geophysics Lab, Hanscomb Air Force Base, MA, AFGL-TR-88-0177.
- Künнемeyer, R., *et al.*, 2001: A simple reflectometer for on-farm pasture assessment. *Computers and Electronics in Agriculture* 31: 125–136.
- Lantinga, E.A., *et al.*, 1999: Modelling and measuring vertical light absorption within grassclover mixtures. *Agricultural and Forest Meteorology* 96: 71–83.
- Larsolle, A. and Hamid Muhammed, H., 2007: Measuring crop status using multivariate analysis of hyperspectral field reflectance with application to disease severity and plant density. *Precision Agriculture* 8, 37–47.

- Lawrence, K.C., *et al.*, 2007: Evaluation of LED and tungsten halogen lighting for fecal contaminant detection. *Applied Engineering in Agriculture* 23 (6), 811–818.
- Lee, K.-S., *et al.*, 2004: Hyperspectral versus multispectral data for estimating leaf area index in four different biomes. *Remote Sensing of Environment* 91, 508–520.
- Lemaire, G. and Gastal, A., 1997: N uptake and distribution in plant canopies. In: Lemaire G, ed. *Diagnosis of the nitrogen status in crops*. Berlin: Springer-Verlag, 3–43.
- Lemmer, A. and Oechsner, H., 2001: Co-fermentation of grass and forage maize. *Landtechnik* 56:412–413.
- Leuning, R., *et al.*, 2006: A multi-angle spectrometer for automatic measurement of plant canopy reflectance spectra. *Remote Sensing of Environment* 103, 236–245.
- Loges, R., 1998: Ertrag, Futterqualität, N<sub>2</sub>-Fixierungsleistung und Vorfruchtwert von Rotklee- und Rotklee grasbeständen. PhD. thesis Univ. of Kiel; Schriftenreihe des Instituts für Pflanzenbau und Pflanzenzüchtung der Christian-Albrecht-Universität zu Kiel, Germany.
- Longe, O.G. and Ogedegbe, N., 1989: Influence of fiber on metabolizable energy of diet and performance of growing pullets in the tropics. *British Poultry Science* 30: 193–196.
- Los, S.O. *et al.*, 2005: A method to convert AVHRR Normalized Difference Vegetation Index time series to a standard viewing and illumination geometry. *Remote Sensing of Environment* 99, 400–411.
- Lovett D.K., *et al.*, 2004: Using near infrared reflectance spectroscopy (NIRS) to predict the biological parameters of maize silage. *Anim Feed Sci Technol* 115:179–187.
- Mahiny, A.S. and Turner, B.J., 2007: A comparison of four common atmospheric correction methods. *Photogrammetric Engineering and Remote Sensing* 74 (4): 361–368.

- Maleki, M.R. *et al.*, (2008): On-the-go variable-rate phosphorus fertilisation based on a visible and near-infrared soil sensor. *Biosystems Engineering* 99: 35–46.
- Martens, H. and Naes, T., 1989: *Multivariate Calibration*. Wiley, Chichester, p 419.
- Meier, U., 2001: Growth stages of mono- and dicotyledonous plants. BBCH monograph (2. ed.). Federal biological research centre for agriculture and forestry, Braunschweig, Germany.
- Miao, Y. *et al.*, 2009: Combining chlorophyll meter readings and high spatial resolution remote sensing images for in-season site-specific nitrogen management of corn. *Precision Agriculture* 10, 45–62.
- Miller, C.E., 2001: Chemical principles of near-infrared technology. In: Williams, P. and K. Norris (Eds.). *Near-infrared technology in the agricultural and food industries* (2. ed. pp. 19-37). American Association of Cereal Chemists, Minesota, USA.
- Milton, E.J. and Goetz, A.F.H., 1997: Atmospheric influences on field spectrometry: observed relationships between spectral irradiance and the variance in spectral reflectance. *Proceedings of the International Conference on Physical Measurements and Signatures in Remote Sensing*, France, Courchevel.
- Mistele, B. and Schmidhalter, U., 2008: Estimating the nitrogen nutrition index using spectral canopy reflectance measurements. *European Journal of Agronomy* 29, 184–190.
- Morón, A., *et al.*, 2007: Preliminary study on the use of near-infrared reflectance spectroscopy to assess nitrogen content of undried wheat plants. *J Sci Food Agric* 87:147–152.
- Moschner C.R. and Biskupek-Korell, B., 2006: Estimating the content of free fatty acids in high-oleic sunflower seeds by near-infrared spectroscopy. *Eur J Lipid Sci Technol* 108:606–613.

- Moschner, C.R., 2007: Methodische Untersuchungen zum Einsatz der Nahinfrarot-Spektroskopie (NIRS) zur Qualitätsbeurteilung von High-Oleic-Sonnenblumen. Doctoral thesis, University of Göttingen, Germany.
- Mutanga, O., *et al.*, 2004: Discriminating sodium concentration in a mixed grass species environment of the Kruger National Park using field spectrometry. *International Journal of Remote Sensing* 25 (20), 4191–4201.
- Nassiri, M. and Elgersma, A., 1998: Competition in perennial ryegrass/white clover mixtures. II. Leaf characteristics, light interception, light interception and dry matter production during regrowth. *Grass and Forage Science* 53, 367–379.
- Naumann C. and Bassler, R. 2004: Methodenbuch Band III Chemische Untersuchungen von Futtermitteln (Book of methods volume III: Chemical analysis of animal feeds). Verband Deutscher Landwirtschaftlicher Untersuchungs- und Forschungsanstalten, 5th edn. VDLUFA-Verlag, Darmstadt.
- Norris, K.H. *et al.*, 1976: Predicting forage quality by infrared reflectance spectroscopy. *Journal of Animal Science* 43: 889–897.
- Noike T., *et al.*, 1985: Characteristics of carbohydrate degradation and the rate-limiting step in anaerobic digestion. *Biotechnol Bioeng* 27:1482–1489
- Numata, I., *et al.*, 2007: Characterization of pasture biophysical properties and the impact of grazing intensity using remotely sensed data. *Remote Sensing of Environment* 109: 314–327.
- Nousiainen J., *et al.*, 2004: Prediction of indigestible cell wall fraction of grass silage by near infrared reflectance spectroscopy. *Anim Feed Sci Technol* 115:295–311.
- Obernberger I., *et al.*, 2006: Chemical properties of solid biofuels—significance and impact. *Biomass Bioenergy* 30:973–982.
- Oppelt, N., 2002: Monitoring of Plant Chlorophyll and Nitrogen Status Using the Airborne Imaging Spectrometer AVIS. Doctoral thesis, University of Munich, Germany.

- Park, R.S., *et al.*, 1997: The use of near infrared reflectance spectroscopy on dried samples to predict biological parameters of grass silage. *Animal Feed Science Technology* 68: 235–246.
- Park R.S., *et al.*, 1998: The use of near infrared reflectance spectroscopy (NIRS) on undried samples of grass silage to predict chemical composition and digestibility parameters. *Anim Feed Sci Technol* 72:155–167.
- Petisco C., *et al.*, 2005: Use of near-infrared reflectance spectroscopy in predicting nitrogen, phosphorus and calcium contents in heterogeneous woody plant species. *Anal Bioanal Chem* 382:458–465.
- Plénet, D. and Lemaire, G., 1999: Relationships between dynamics of nitrogen uptake and dry matter accumulation in maize crops. Determination of critical N concentration. *Plant and Soil* 216, 65–82.
- Pordesimo, L. O. *et al.*, 2005: Variation in corn stover composition and energy content with crop maturity. *Biomass and Bioenergy* 28, 366–374.
- Price, K.P., *et al.*, 2002: Comparison of Landsat TM and ERS-2 SAR data for discriminating among grassland types and treatments in eastern Kansas. *Computers and Electronics in Agriculture* 37, 157–171.
- Prochnow A., *et al.*, 2005: Seasonal pattern of biomethanisation of grass from landscape management. In: *Agricultural Engineering International: the CIGR E-journal*, Vol. VII, Manuscript EE 05 011, <http://cigrjournal.org/index.php/Ejournal> (accessed 2 January 2009).
- Qi, J., *et al.*, 1995: Normalization of sun/view angle effects using spectral albedo-based vegetation indices. *Remote Sensing of Environment* 52 (3): 207–217.
- Rees, W.G., *et al.*, 2004: Reflectance spectra of subarctic lichens between 400 and 2400 nm. *Remote Sensing of Environment* 90, 281–292.
- Reeves J., *et al.*, 2002: The potential of diffuse reflectance spectroscopy for the determination of carbon inventories in soils. *Environ Pollut* 116:S277–S284.

- Reulein J., *et al.*, 2007: Efficient utilization of biomass through mechanical dehydration of silages. In: Proceedings of the 15th European Biomass Conference & Exhibition, Germany, pp 1770–1774
- Reusch, S., 1997: Entwicklung eines reflexionsoptischen Sensors zur Erfassung der Stickstoffversorgung landwirtschaftlicher Kulturpflanzen. Forschungsbericht Agrartechnik 303. Doctoral thesis, University of Kiel, Germany.
- Reusch, S., 2003: Optimisation of oblique-view remote measurement of crop N-uptake under changing irradiance conditions. In: J. V. Stafford & A. Werner (Eds.), Proceedings of the 3rd European Conference on Precision Agriculture, The Netherlands, Wageningen Academic Publishers, pp. 573–578.
- Reusch, S., 2005: Optimum waveband selection for determining the nitrogen uptake in winter wheat by active remote sensing. In: J. V. Stafford (Ed.), Proceedings of the 5th European Conference on Precision Agriculture, The Netherlands, Wageningen Academic Publishers, pp. 261–266.
- Richter, R., 1996: A spatially adaptive fast atmospheric correction algorithm. *International Journal of Remote Sensing* 17 (6), 1201–1214.
- Richter, F., *et al.*, 2009b: Utilization of semi-natural grassland through integrated generation of solid fuel and biogas from biomass. III. Effects of hydrothermal conditioning and mechanical dehydration on solid fuel properties and on energy and green house gas balances. *Grass & Forage Science*, submitted.
- Ruano-Ramos A, *et al.*, 1999a: Near infrared spectroscopy prediction of mineral content in botanical fractions from semi-arid grasslands. *Anim Feed Sci Technol* 77:331–343.
- Ruano-Ramos A., *et al.*, 1999b: Determination of nitrogen and ash contents in total herbage and botanical components of grassland systems with near infra-red spectroscopy. *J Sci Food Agric* 79:137–143.
- Rudzik, L., 1993: Infrarotfibel. Infrarotspektroskopie für die Lebensmittel- und Milchindustrie. B. Behrs Verlag, Hamburg, Germany.



- Salazar, L. *et al.*, 2008: Using vegetation health indices and partial least squares method for estimation of corn yield. *International Journal of Remote Sensing* 29 (1), 175–189.
- Sandmeier, St. *et al.*, 1998: Physical Mechanisms in Hyperspectral BRDF Data of Grass and Watercress. *Remote Sensing of Environment* 66, 222–233.
- SAS Institute (2002 – 2008): SAS version 9.2. SAS Institute. Cary, NC, USA.
- Savitzky, A. and Golay, M.J.E., 1964: Smoothing and differentiation of data by simplified least squares procedures. *Analytical Chemistry* 36: 1627–1639.
- Schade, N., *et al.*, 2007: Enhanced solar global irradiance during cloudy sky conditions. *Meteorologische Zeitschrift* 16 (3), 295–303.
- Schilling, G., 2000: *Pflanzenernährung und Düngung*. Ulmer, Stuttgart.
- Schino, G., *et al.*, 2003: Satellite estimate of grass biomass in a mountainous range in central Italy. *Agroforestry Systems* 59: 157–162.
- Schmidt, K.S. and Skidmore, A.K., 2003: Spectral discrimination of vegetation types in a coastal wetland. *Remote Sensing of Environment* 85, 92–108.
- Schmidt, J.P., *et al.*, 2009: Nitrogen Recommendations for Corn: An On-The-Go Sensor Compared with Current Recommendation Methods. *Agronomy Journal* 101 (4), 914–924.
- Segal, M. and Davis, J., 1992: The Impact of Deep Cumulus Reflection on the Ground-Level Global Irradiance. *Journal of Applied Meteorology* 31, 217–222.
- Senay, G.B. *et al.*, 2000: Using High Spatial Resolution Multispectral Data to Classify Corn and Soybean Crops. *Photogrammetric Engineering & Remote Sensing* 66 (3), 319–327.
- Serrano, L., *et al.*, 2000: Remote Sensing of Biomass and Yield of Winter Wheat under Different Nitrogen Supplies. *Crop Science* 40, 723–731.
- Shiralipour A. and Smith, P.H., 1984: Conversion of biomass into methane gas. *Biomass* 6:85–92.

- Starks, P.J., *et al.*, 2008: Estimation of nitrogen concentration and in vitro dry matter digestibility of herbage of warm-season grass pastures from canopy hyperspectral reflectance measurements. *Grass and Forage Science* 63: 168–178.
- Stülpnagel R., *et al.*, 1992: Investigations for a cheap estimation of the net calorific values (n.c.v.) of different biomasses. 7th European Conference on Biomass for Energy and Environment, Agriculture and Industry, Florence, Italy.
- Stülpnagel R., *et al.*, 2008: Fortschritte im Bereich der energetischen Wandlung von landwirtschaftlichen Kulturpflanzen durch erweiterte Analytik des Erntegutes (Progress in the area of energetic conversion of agricultural crops by enhanced analysis of the harvest). In: DGMK-Fachtagung Energetische Nutzung von Biomassen, pp 199–206, Velen, Germany, 2008.
- Stuth J, *et al.*, 2003: Direct and indirect means of predicting forage quality through near infrared reflectance spectroscopy. *Field Crops Res* 84:45–56
- Tachiiri, K., 2005: Calculating NDVI for NOAA/AVHRR data after atmospheric correction for extensive images using 6S code: A case study in the Marsabit District, Kenya. *ISPRS Journal of Photogrammetry & Remote Sensing* 59, 103–114.
- Terhoeven-Urselmans, T., *et al.*, 2006: Near-infrared spectroscopy can predict the composition of organic matter in soil and litter. *Journal of Plant Nutrition and Soil Science* 169: 168–174.
- Thenkabail, P.S., *et al.*, 2000: Hyperspectral vegetation indices and their relationships with agricultural crop characteristics. *Remote Sensing of Environment* 71: 158–182.
- Thorp *et al.*, 2008: Using aerial hyperspectral remote sensing imagery to estimate corn plant stand density. *Transactions of the ASABE*, 51: 311–320.
- Todd, S.W., *et al.*, 1998: Biomass estimation on grazed and ungrazed rangelands using spectral indices. *International Journal of Remote Sensing* 19: 427–438.

- Toonen M.A.J., *et al.*, 2004: Predicting the chemical composition of fibre and core fraction of hemp (*Cannabis sativa* L.). *Euphytica* 140:39–45.
- Tucker, C.J., 1977: Spectral Estimation of Grass Canopy Variables. *Remote Sensing of Environment* 6: 11–26.
- Valdés C., *et al.*, 2006: Potential use of visible and near infrared reflectance spectroscopy for the estimation of nitrogen fractions in forages harvested from permanent meadows. *J Sci Food Agric* 86:308–314.
- Vermote, E.F., *et al.*, 1997: Second simulation of the satellite signal in the solar spectrum, 6S: An overview. *IEEE Transactions on Geoscience and Remote Sensing* 35 (3), 675–686.
- Volkers K.C., *et al.*, 2003: Prediction of the quality of forage maize by near-infrared reflectance spectroscopy. *Anim Feed Sci Technol* 109:183–194.
- Wachendorf M., *et al.*, 2009: Utilisation of semi-natural grassland through an integrated generation of solid fuel and biogas from biomass. Part I: Effects of hydrothermic conditioning and mechanical dehydration on mass flows of organic and mineral plant compounds and nutrient balances. *Grass Forage Sci* 64:132–143
- Walter-Shea, E.A., *et al.*, 1997: Relations between directional spectral vegetation indices and leaf area and absorbed radiation in alfalfa. *Remote Sensing of Environment* 61, 162–177.
- Wörner, H., 1972: Die Berechnung der Globalstrahlung aus Trübungswert und Bewölkung. *Pure and Applied Geophysics* 93 (1), 177–186.
- Wu J.G., *et al.*, 2002: Estimating the amino acid composition in milled rice by near-infrared reflectance spectroscopy. *Field Crops Res* 75:1–7.
- Wylie, B.K., *et al.*, 2002: Satellite mapping of surface biophysical parameters at the biome scale over the North American grasslands, a case study. *Remote Sensing of Environment* 79, 266–278.

- Xavier, A.C., *et al.*, 2006: Hyperspectral field reflectance measurements to estimate wheat grain yield and plant height. *Scientia Agricola* 63 (2), 130–138.
- Xiccato G., *et al.*, 2003: Prediction of chemical composition, nutritive value and ingredient composition of European compound feeds for rabbits by near infrared reflectance spectroscopy (NIRS). *Anim Feed Sci Technol* 104:153–168.
- Zangvil, A. and Lamb, P.J., 1997: Characterization of sky conditions by the use of solar radiation data. *Solar Energy* 61 (1), 11–22.
- Zwiggelaar, R., 1998: A review of spectral properties of plants and their potential use for crop/weed discrimination in row-crops. *Crop protection* 1: 189–206.